
# Measuring Mitochondrial Dysfunction in Humans

By Mark J Brinsden

A thesis submitted for the degree of

Bachelor of Biomedical Science with Honours

University of Otago, Christchurch

October, 2015

# Abstract

Mitochondria are essential organelles found in almost every cell in the human body. They host a number of important metabolic pathways and carry out essential biological functions such as ATP synthesis and regulating cell death. There is a slow decline in mitochondrial function associated with ageing and mitochondrial dysfunction is proposed to act causally in a number of diseases. Previously it has been difficult to measure the health of human mitochondria as tests have required tissue from invasive muscle biopsies. The Seahorse XF Analyser is a recent technological advance that enables researchers to test mitochondrial function in small numbers of live cells. Recently, using the Seahorse analyser, peripheral blood cells such as platelets, monocytes and lymphocytes have been shown to display individually distinct bioenergetic profiles. During circulation, these cells are exposed to metabolic or environmental stressors throughout the body, potentially allowing them to act as biomarkers of bioenergetic health and ageing. Different cell preparations were trialled to purify and isolate platelets, monocytes and lymphocytes from freshly drawn whole blood. These protocols succeeded in preparing platelet and T-lymphocyte samples for XF analysis, however inconsistent results indicated that the protocols need further development. The Seahorse XF analyser was used to measure bioenergetic function in human platelets and T-lymphocytes from healthy donors ranging from 21 to 56 years of age. Each cell type required optimisation experiments to determine the optimal inhibitor and substrate concentrations to generate a meaningful bioenergetic profile. Similarly, seeding densities were determined to ensure oxygen consumption values that were suitable to the instruments sensitivity. These cell types have elastic metabolic phenotypes, and appeared sensitive to metabolic switching during early stages of the XF assay. Platelets were particularly difficult to work with because of their inclination to cease using oxidative phosphorylation and switch metabolism to using purely glycolytic pathways. Platelet susceptibility for metabolic switching is undetermined at this point. Lymphocyte optimization experiments also indicated possible premature activation during the assay. Further work is needed to fine tune this protocol to ensure consistent and uniform measurements before accurate BHI values are calculated for donors of different ages.

# Acknowledgements

First I would like to express my gratitude to my supervisors Dr Andree Pearson and Professor Mark Hampton for their support, leadership and guidance throughout my project and for always finding time amongst your full and busy lives. Thanks for all your hard work and patience with me and for teaching me so many skills throughout this year. Thanks for making the free radical lab a great learning environment and instilling a friendly and thoughtful culture among the group.

I am also very grateful to the Barry Hock and Judy McKenzie from the Haematology Research Group. Thanks for allowing me to pester you all year long and for giving me access to the instruments and materials in your labs. Thanks also to William Titulaer for his help and worldly advice.

Thank you Dr Karina O'Connor for finding time to lend us all a hand and for your previous efforts laying the groundwork for all Seahorse users.

I am grateful to all the CFRR staff and students who provided me with support, suggestions and guidance on all things Science, and for being so approachable, friendly and helpful.

To all the kind people who donated blood for this project I am extremely grateful.

I would finally like to thank my fellow BBiomedSci(hons) students for an enjoyable year and wish them all the best in all future endeavours. Thanks and well done to you all.

# List of abbreviations

| | |
|---|---|
| AD | Alzheimer's disease |
| AMA | Antimycin A |
| ATP | Adenosine triphosphate |
| BHI | Bioenergetic health index |
| BSA | Bovine Serum Albumin |
| DMEM | Dulbecco's modified eagle medium |
| DNA | Deoxyribonucleic acid |
| EDTA | Ethylenediamine-tetraacetic acid |
| ETC | Electron transport chain |
| FCCP | Carbonyl cyanide p-trifluoromethoxyphenylhydrazone |
| FBS | Fetal bovine serum |
| GL | Glycolysis |
| GLN | Glutamine |
| $H_2O_2$ | Hydrogen peroxide |
| mAb | Monoclonal antibody |
| MACS | Magnetically activated cells sorting |
| mtDNA | Mitochondrial DNA |
| NADH | Nicotinamide adenine dinucleotide |
| nDNA | Nuclear DNA |
| NK | Natural killer |
| OCR | Oxygen consumption rates |
| OLI | Oligomycin |
| OXPHOS | Oxidative phosphorylation |
| PBS | Phosphate buffered saline |
| $PGI_2$ | Prostacyclin |
| PMF | Proton motive force |
| RBC | Red blood cell |
| PRP | Platelet rich plasma |
| ROS | Reactive oxygen species |
| RPMI | Roswell Park Memorial Institute medium |

| | |
|---|---|
| RT | Room temperature |
| SCD | Sickle cell disease |
| SOD | Superoxide dismutase |
| TCA | Tricarboxylic acid |
| TRIS | Tris (hydroxymethyl)aminomethane |
| T2DM | Type 2 diabetes mellitus |
| XF | Extracellular flux |

# Table of Contents

# List of Figures

# List of Tables

# Chapter One: Introduction

## 1.1 Overview

A mitochondrion is a discrete double-membrane-bounded organelle found in all eukaryote organisms, a group which encompasses all plants, animals, fungi and protists (1). A binding relationship was forged with these intracellular symbionts during a chapter of the eukaryote's greatly-distant evolutionary past (2). Consequently, these cellular residents now inhabit all human cells, with the only exception being erythrocytes (3). In humans, the most prolific role of mitochondria is the synthesis of adenosine triphosphate (ATP), a ubiquitous energy storage molecule of the cell. ATP synthesis requires a coordinated set of biochemical reactions which occur in and around the mitochondrial inner membrane in a process known as oxidative phosphorylation (OXPHOS). Central to the OXPHOS system is a chemical reaction which involves the reduction of molecular oxygen to water making OXPHOS, the predominant consumer of the oxygen we breathe and the major component of cellular respiration (4). In addition to ATP synthesis, mitochondria play host to a number of important metabolic pathways - the tricarboxylic acid (TCA) cycle, β-oxidation, lipid and cholesterol synthesis – as well as regulating cell death and carrying out intracellular signalling through the production of reactive oxygen species (ROS) (5, 6). Mitochondria are organelles of power and influence whose function is fundamental to the cell life and death.

The central components of OXPHOS are illustrated in Figure 1. Four protein complexes - labelled I through IV - are known collectively as the electron transport chain (ETC). Three of these complexes combine substrate reactions with the pumping of protons from the mitochondrial matrix to the intermembrane space. Complex II, while incapable of proton pumping, facilitates electron transfer within the transport chain. Electrons are donated through oxidation of nicotinamide adenine dinucleotide (NADH) and succinate, which are endogenous substrates generated from the TCA cycle. The terminal electron acceptor of the ETC is molecular oxygen, which is subsequently reduced to form $H_2O$ at complex IV. The directional pumping of proton ions into the intermembrane space creates a proton motive force (PMF) across the inner membrane in the order of 200 mV (7). A proton circuit is formed when the PMF drives protons re-entry into the matrix through a

transmembrane ATP synthase. Proton passage provides the energy to release a newly phosphorylated ATP from the catalytic domain of the synthase protein. Together, these bioenergetic transformations form a tightly coupled system which can be measured by monitoring oxygen reduction occurring at complex IV. As such, the OXPHOS system is measured indirectly by measuring cellular respiration (8).

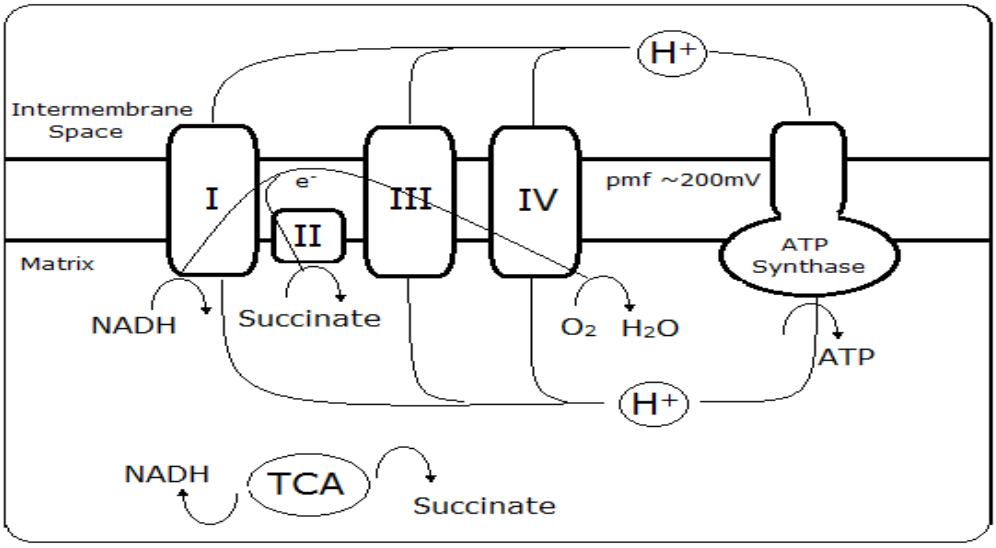


***Figure 1.1 Oxidative phosphorylation and the proton circuit of the mitochondrial inner membrane****: Protons are pumped into the intermembrane space by complexes I, III and IV and return via the ATP synthase, generating ATP. The proton circuit is coupled with the oxidation of substrates (NADH and succinate) and electron transfer through the electron transport chain which terminates with the reduction of molecular oxygen to water at complex IV.* *Source: Mark J Brinsden*

## 1.2 Mitochondrial Damage

Mitochondria numbers within a cell type are variable and dynamic. The population flux is managed by the contrasting biological processes of biogenesis and mitophagy, the latter being the non-random mitochondrial degradation by autophagy (9). Biogenesis involves the growth and division of pre-existing mitochondria. Due to their unique origin, mitochondria contain their own genome, which exists as numerous copies of circular double-stranded mitochondrial DNA (mtDNA) molecules and can number in the thousands per cell (10, 11). The great majority of mitochondrial proteins are encoded by nuclear DNA (nDNA); however, an important subset is still encoded by the mitochondria's own genome. Successful biogenesis requires mtDNA replication and the synthesis and transport of thousands of necessary proteins (12). These multitudes of proteins and DNA components are each susceptible to damage. As mtDNA has no histone proteins, mutations accumulate 10-20 times faster than in nuclear genes (13), though mutations in either DNA type can greatly effect mitochondrial function.

Protein complexes I, II, and III of the ETC contain reactive sites where unpaired electrons can leak onto molecular oxygen, forming superoxide anion radical $O_2^-$ (5). This free radical species can rapidly dismutate to hydrogen peroxide ($H_2O_2$) in a reaction that can occur spontaneously or be catalysed by the enzyme superoxide dismutase (SOD) (5). It is estimated that mitochondria are responsible for the majority (~90%) of cellular ROS production (14). ROS can cause lipid peroxidation and oxidative damage to surrounding membranes and biomolecules (15), meaning locally generated ROS can directly damage any of the ETC proteins, TCA cycle enzymes and nuclear or mtDNA (16). Thus mitochondria are both a major source and target of ROS damage (17). The ongoing confrontation of oxidative damage is emphasised by the extensive array of antioxidant defences present in mitochondria (10). Despite these defences, mitochondria have the potential to perpetuate oxidative damage, which contributes to their own damage and dysfunction. Without adequate mitophagy, damaged or dysfunctional mitochondria contribute further ROS production and oxidative stress that may lead to damage and dysfunction of surrounding cellular components. A declining turnover rate of dysfunctional cellular components is considered to contribute to the deterioration of tissues and organs seen with ageing (18), hence the orderly turn-over of damaged

mitochondria is critical to limit these undesirable effects of ageing (9). Unsurprisingly, dysfunctional mitochondria and deficient mitophagy have been suggested as leading causes of aging due to the resulting increase in mtDNA mutations and oxidative stress (10, 14, 19, 20). As such, mitophagy has recently garnered interest in ageing and longevity studies (21).

## 1.3 Mitochondrial Dysfunction and Disease

Given their ubiquitous presence and precarious biology, it seems intuitive that dysfunctional mitochondrial will play a role in disease. The archetypal mitochondrial diseases cause obvious and chronic debilitation in sufferers. These diseases are genetic disorders caused by defects in mitochondrial or nuclear DNA and may be either inherited or arise through spontaneous biological damage (10, 22). Historically these diseases have been identified and classified by the dominant disablement they cause (23). The best known are mitochondrial myopathies, which have been recognized since the 1960s as a collection of syndromes with common symptoms of muscle weakness and exercise intolerance (24).

Aside from chronic mitochondrial diseases, mtDNA mutations are also observed to occur in other human diseases, including colon and prostate cancer (25, 26), positing the question of whether mitochondrial dysfunction may play a causal role in these diseases. Dysfunctional mitochondria have therefore become a focal point in the investigation into common human diseases. The same self-perpetuating damage and dysfunctions thought responsible for the ageing process are also believed to contribute to age-related neurodegenerative disorders such as Alzheimer's disease (AD) (27). In fact, there is evidence that mitochondrial dysfunction not only occurs early in all types of neurodegenerative disease, but also acts causally in the pathogenesis of these diseases (10).

Based on the notion that failure to remove damaged mitochondria will cause deterioration in bioenergetics function (28), a recent trend in translational research has been to investigate bioenergetic dysfunction in disease sufferers. Energetic abnormalities

have been demonstrated in a host of common and progressive diseases, including diabetes (29), neurodegeneration (10, 19), cardiovascular disease (30) and cancer (31, 32). These studies identify varying abnormalities between diseased and healthy controls without positing a causative mechanism. They do, however, bolster the notion that mitochondrial dysfunction may play a greater role in human disease than is currently recognized.

## 1.4 Measuring Mitochondrial Dysfunction

Abnormality in any of the biological processes that mitochondria perform can be considered mitochondrial dysfunction. Frequently, however, dysfunction is measured in terms of the canonical role of ATP synthesis by OXPHOS. As OXPHOS is central to many of the physiological functions of the mitochondria it provides a critical measure to encompass a wide variety of dysfunctions (33). Two predominant measurement types are employed to measure the OXPHOS: 1 - quantify the potential of the PMF, and 2 - quantify the proton flux or 'current' through the system. The proton current is measured indirectly via the reduction of molecular oxygen at complex IV, made possible due to the tight coupling of the reactions of the ETC complexes and proton pumping into the mitochondrial intermembrane space. This relationship holds for both isolated mitochondria and cells (34).

The earliest methods of measuring oxygen consumption used a Clarke-type oxygen electrode (35) that was developed by Chance and Williams to measure OXPHOS of isolated mitochondria in suspension (36). In these classical experiments, mitochondria are isolated, purified and subsequently incubated in suspension under different substrate and extracellular conditions in order to measure defined respiration states. Assays were restricted to cells which could be obtained in high yields, and as a result, nervous tissue and liver cells were the main sources for samples used in assays (37, 38). Despite the sample limitations, experiments were able to measure a range of OXPHOX components, including substrate transport and metabolism, electron delivery to the ETC, the activities

of protein complexes, ATP synthesis, proton leak and more (33). Collectively these measurement parameters came to represent mitochondrial bioenergetics.

The preceding years saw many developments in the technology of measuring oxygen consumption. Cell respirometers using coverslip-attached cells incorporated continuous monitoring of the cellular respiration (39). This technology employed an isolated ~130-µl volume chamber with polarographic oxygen electrodes at both the inlet and outlet ports of the chamber. These dynamic measures made oxygraphy – traces of oxygen consumption over time – the representative measure of mitochondrial bioenergetics. Concurrently, assays were developed using 96 well plates integrated with fluorescent sensors (40). Meanwhile, the Oroboros, a benchtop micro-respirometer, greatly advanced software and calibration procedures (41). Together these technical advances set the scene for development of the Seahorse Bioscience extracellular flux (XF) analyser shown below in Figure 1.2.


***Figure 1.2 The Seahorse Bioscience XFe24 analyser.***

*Source: http://www.seahorsebio.com/learning/image-library.php*

The Seahorse instrument uses fluorimeters to detect dissolved oxygen ($O_2$) and free proton concentration (H+) in the extracellular media. This is performed by pairs of solid state probes built into a sensor cartridge which sits above and covers the multi-well microplate that contains the samples (Figure 1.3). The cartridge sensors are

automatically lowered to 200 microns from the well bottom during each measurement cycle, creating a transient 7 µl volume chamber from within which changes in real-time $O_2$ and H+ concentration are measured [17]. Measuring the change in these concentrations over a prescribed time-frame gives either the oxygen consumption rate (OCR, pmol/min) or extracellular acidification rate (ECAR, mpH/min). The cartridge also contains four injection ports per sample well, allowing for the introduction of soluble additives to each well at desired points during the assay. The multi-well, automated, high throughput assay allows versatility in experimental design. It may be used on intact viable whole cells [17] or on isolated mitochondria [37], and permits the ability to measure OXPHOS in a more physiologically relevant context.

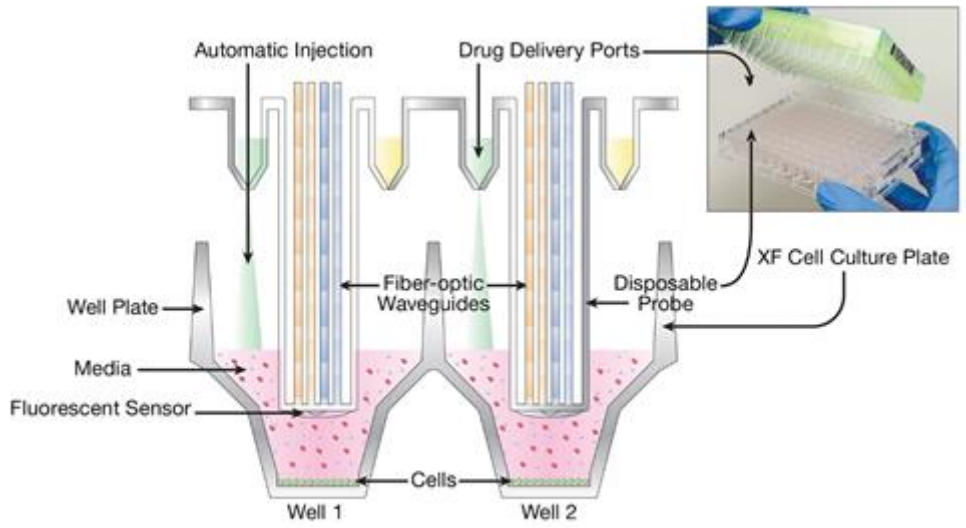


***Figure 1.3 How the XF instrument works****: The Seahorse instrument uses retractable probes and inbuilt delivery ports to facilitate dynamic measurement of $O_2$ and $H^+$ concentrations. Source: http://www.seahorsebio.com/learning/image-library.php*

## 1.5 Mitochondrial Stress Test and Bioenergetic Health Index

The mitochondrial stress test is a protocol for measuring mitochondrial bioenergetic function using the Seahorse XF analyser (Figure 1.4). During a stress test the OCR of a cell population is measured at consecutive time points and under varying conditions brought about by the addition of modulators to the extracellular media. Once a stable basal respiration rate is established the drug oligomycin (Oli) is introduced to inhibit the ATP synthase by blocking proton passage. The resulting decrease in OCR reveals the respiration previously attributable to ATP production. Next the ionophore FCCP (carbonyl cyanide p-trifluoromethoxyphenylhydrazone) is introduced to uncouple the proton gradient across the inner mitochondrial membrane from the pumping of protons by the ETC. FCCP is a mobile ion carrier that allows pumped protons to rapidly cycle from the intermembrane space back into the mitochondrial matrix. The resulting depolarisation of the inner membrane allows the ETC components to operate at a greater rate, resulting in an OCR measurement that represents the maximal mitochondrial respiration rate. The difference in OCR between the maximal and basal measurements is termed the spare reserve capacity and is used to measure the ability of OXPHOS to accommodate rapid rises in metabolic demand (42). Finally, an inhibitor of the ETC (antimycin A) is introduced to stop the reduction of oxygen occurring at complex IV. The residual OCR is deemed attributable to non-mitochondrial respiration and is subtracted from all other measures. This modulator also allows for measurement of proton leak occurring across the inner–membrane.

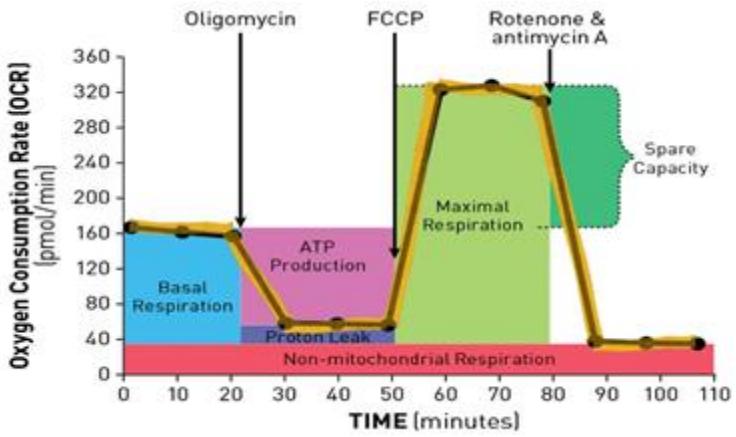


***Figure 1.4 The mitochondrial stress test.***

*Source: http://www.seahorsebio.com/learning/image-library.php*

To capitalise on the ability of the mitochondrial stress test to measure multiple aspects of mitochondrial bioenergetics, Chacko *et al.* (2014) proposed integrating the critical measurement parameters into a single metric which they termed the bioenergetic health index (BHI) (28). This single composite value (Figure 1.5) could be used to monitor and compare a person's mitochondrial function over time and potentially to make comparisons between individuals.

$$\mathrm{BHI} = \log \frac{(\text{reserve capacity})^a \times (\text{ATP-linked})^b}{(\text{non-mitochondrial})^c \times (\text{proton leak})^d}$$

***Figure 1.5 The bioenergetic health index***

## 1.7 Measuring Mitochondrial Bioenergetics in Human Blood Cells

To screen human populations an easily accessible source of mitochondria is required. The Seahorse XF analyser allows for bioenergetic measurement of intact cells sourced from a host of tissue samples or cell cultures. One such source has been cells isolated from freshly drawn whole blood. Of these, platelets have tended to be the popular choice of sample for XF analysis since the introduction of the Seahorse instrument (43-45). This is due in part to their abundance and distribution throughout the circulatory system. Platelets are anucleate cells and so provide a model with a much diminished scope for mitochondrial repair and biogenesis.

A study by Avila *et al.* (2011) used platelet mitochondria as a biological sensor to investigate the systemic effects of Type 2 diabetes mellitus (T2DM) (43). XF analysis using the Seahorse revealed platelets in the T2DM cohort to have diminished oxygen consumption and ATP turnover when compared to the insulin sensitive control group (n=8). Further investigations showed up-regulation of mitochondrial anti-oxidant enzymes, which was described by the author as a 'stress-signature' of the disease. It was suggested that this phenomenon is possibly due to the platelets' exposure to oxidative

stresses early on in their life cycle while they are present in the bone marrow compartment. Despite the relatively small sample size, these findings highlight the use of blood cells as a surrogate for assessing the systemic effects of disease in remote parts of the human body. This idea has become known as the biological 'canary in the coal mine' (46).

The scope of the XF analysis was validated in a 2014 study by Cardenes *et al.* (44). In this work, platelet bioenergetics were measured in patients with sickle cell disease (SCD) and subsequently compared against control measurements taken from a healthy population. SCD patients are known to exhibit aberrant platelet activation, but the mechanism remains unknown. XF analysis revealed a significant decrease in basal respiration (~30%) and proton leak (~32%). A subsequent enzyme activity assay then identified a marked decrease in ATP synthase activity (~36%) despite protein expression assay being similar in both groups. The group then conducted further experimentation to show significant correlation between the bioenergetic alteration and aberrant platelet activation, suggesting a causal relation. In addition, it was demonstrated that - when normalised to cell count - the data from XF analysis is consistent with Clarke electrode assay and that the percentage of activated platelets did not change from before and after the XF experiment. Cardenes *et al.*'s study demonstrates the investigative potential of XF analysis when conducted on cells isolated from easily obtained blood samples. While it must be recognised that the cell type was known to be dysfunctional, the cohort provides an effective positive control for this type of study.

In 2015 a number of experiments have been published which use XF analysis on platelets to measure mitochondrial function. The mitochondrial stress test and BHI have been used to test and compare the bioenergetic performance of fresh isolated compared with stored platelets (47), and platelets have been used to demonstrate a systemic metabolic alteration in asthma patients (48). Significant new research has investigated the effects of both thrombin activation and glutamine supplementation on platelets (49).

Perhaps in a follow up of Avila *et al.'s* research (43), Hartman *et al.* (2014) used XF analysis to assay peripheral blood mononuclear cells (PBMC) in T2DM patients (50). This research group used a mixture of PBMCs isolated through centrifugation and layer separation. Fluorescence activated cell sorting (FACS) revealed that samples obtained by this method contained 82% lymphocytes and 14% monocytes. Results showed that OCR was higher for basal and maximal respiration measurements in diabetic patients compared to control. The group also go on to demonstrate a pattern of mitochondrial oxygen consumption consistent with higher production of reactive oxygen species. While the benefits of testing a mixture of PBMCs are unclear, this study shows a development of the blood cell assay concept by testing lymphocytes and monocytes.

Around a similar time the utility of assaying blood cell types separately was investigated by Chacko *et al.* (2013). In this methods paper the group established that each of four cell types has both distinct bioenergetics and distribution of ETC complexes (51). Neutrophils were shown to have comparatively low OCR when compared to platelets, monocytes and lymphocytes, and were found to be relatively unresponsive to modulation factors typical of these assays. These two studies nicely validate the use of monocytes and lymphocytes along with platelets in XF analysis of mitochondrial bioenergetic function.

Following multiple studies measuring mitochondrial function in PBMCs or platelets (43-45, 50, 52) a comprehensive protocol was recently published by Kramer *et al.* (2014) which outlines methods to isolate, purify and measure the bioenergetics of four peripheral blood cell types (53). This assay was designed to be conducted on a single 20 ml sample of freshly collected blood and serves as a proof of concept that parallel XF experiments may be used as a clinical assay to measure bioenergetic dysfunction. Also included in this report is cursory data from 6-8 healthy donors, which serves as a guideline for replication of this methodology. The authors again expound the idea of using these cell types as surrogates or 'biomarkers' for global metabolic changes, and indicate the potential of this approach in adding prognostic or diagnostic value.

## 1.8 Summary

Mitochondria are a source of ROS that can cause oxidative damage to themselves or surrounding biomolecules. Damaged mitochondria if not adequately recycled can propagate further oxidative damage, and in so doing may be contributing to the pathogenesis of disease and ageing. The Seahorse XF analyser allows dynamic measurement of mitochondrial bioenergetic function in peripheral blood cells isolated from small samples of freshly drawn whole blood. Each blood cell has distinct lifecycles and energetic profiles. They are exposed to systemic metabolic and inflammatory stressors during their maturation and circulation. Measuring their bioenergetic function may offer insight into oxidative damage and disease occurring throughout the body. By combining individual bioenergetic parameters into a single index, it may be possible to measure and compare an individual's mitochondrial function and to make a quick and basic diagnosis of mitochondrial dysfunction.

## 1.9 Thesis Aims

1. To use the mitochondrial stress test to assay mitochondrial bioenergetics of peripheral blood cells (platelets, monocytes and lymphocytes) from individuals constituting a healthy control population, and to use this data set to compile a representative BHI for each distinct cell type.
2. To investigate age related variation in measured bioenergetic parameters and BHI.

# Chapter Two: Materials and Methods

## 2.1 Materials

***Table 2.1. Materials used in this thesis***

| **Antibodies:** | **Supplier** | **Location** |
|---|---|---|
| CD3-PE (UCHTi) | Beckman Coulter | Brea, CA, USA |
| L243 (HLA-DR) | ATCC | Rockville, MD, USA |
| OKMI (CD11B) | ATCC | Rockville, MD, USA |
| Goat Anti-Mouse IgG MicroBeads | Miltenyi Biotech | Bergisch-Gladbach, Germany |
| MACS nanoparticles | Miltenyi Biotech | Bergisch-Gladbach, Germany |
| | | |
| **Media:** | | |
| RPMI (1640) | Sigma-Aldrich | St Louis, MO, USA |
| XF Assay Medium (2mM GlutaMAX™) | Seahorse Biosciences | North Billerica, MO, USA |
| XF Base Medium (no glutamine) | Seahorse Biosciences | North Billerica, MO, USA |
| | | |
| **Modulator Drugs:** | | |
| Antimycin A | Sigma-Aldrich | St Louis, MO, USA |
| FCCP | Sigma-Aldrich | St Louis, MO, USA |
| Oligomycin | Sigma-Aldrich | St Louis, MO, USA |
| Prostacyclin ($PGI_2$) | Sigma-Aldrich | St Louis, MO, USA |
| | | |
| **Seahorse Consumables:** | | |
| XF Calibrant Solution | Seahorse Biosciences | North Billerica, MO, USA |

| | | |
|---|---|---|
| XF24 Cell Culture Microplates | Seahorse Biosciences | North Billerica, MO, USA |
| XF24Sensor Cartridge | Seahorse Biosciences | North Billerica, MO, USA |
| | | |
| **Miscellaneous:** | | |
| Tris | Sigma-Aldrich | St Louis, MO, USA |
| Triton X | Bio-Rad Laboratories | Hercules, CA, USA |
| Cell Tak™ | Corning Incorporated Life Sciences | Tewksbury, MA, USA |

### 2.1.1 Buffers and Media

**Lysis Buffer:** 10 ml Triton® X-100 (final concentration 1% Triton® X-100 in buffer), 10 ml of 1M Tris, 980 ml sterile $H_2O$.

**RPMI-1640**: Supplement with 0.3 g/L L-glutamine.

**XF Base Medium** (minimal DMEM): contains no sodium bicarbonate (buffering agent), glucose, glutamine/GlutaMAX™, or sodium pyruvate.

**XF Assay Medium:** modified DMEM, 0mM Glucose, 2 mM L-Glutamine

**XF-DMEM**: XF assay medium with supplemented with 25 mM D-glucose, 1 mM pyruvate and 2 mM L- glutamine.

## 2.2 Methods

### 2.2.1 Cell Preparation Protocols

All preparations were performed in accordance with aseptic techniques.

#### Platelets

Venous blood was drawn into 9 ml EDTA vacuum tubes and the first 2 ml of blood was discarded to avoid artificial activation due to venepuncture. Platelets were isolated by differential centrifugation as follows: Whole blood was centrifuged with a room temperature (RT) swinging-bucket rotor at 500 x g for 15 min with brake 5/acceleration 0 (B5/A0). Platelet rich plasma (PRP) was collected and allowed to sit for 30 min (RT) before pelleting by centrifugation at 750 x g 10 min (B9/A5). The plasma was removed and the pellet re-suspended in 5 mL of PBS supplemented with 1 µg/mL prostacyclin ($PGI_2$). The suspension was washed by centrifugation at 750 x g 10 min (B9/A5) and re-suspended into 1 mL of PBS+$PGI_2$. Platelet count was determined by turbidimetry using a spectrophotometer (800 nm) as described by Walkowiak *et al.* (54). The volume corresponding to the desired concentration was pelleted by centrifugation at 500 x g 5 min (B9/A5) and re-suspended in the appropriate volume of warm sterile XF base media.

#### Peripheral Blood Mononuclear Cells (PBMCs)

Venous blood was drawn into 9 ml EDTA vacuum tubes and centrifuged with a swinging-bucket rotor at 500 x g for 15 min with brake 5 after which the PRP was collected. The PBMC layer was transferred to sterile 50 ml conical tubes and diluted 4x with basal RPMI. Diluted blood was overlaid onto 15 ml of Ficoll (RT) and centrifuged at 1000 x g for 20 min (B5/A0). The middle band containing PBMCs was carefully collected without disturbing the surrounding bands and diluted 4x with basal RPMI. The suspension was centrifuged at 700 x g 10 min (B9/A5), re-suspended in 1 ml RPMI containing 5% FCS

(RPMI-FCS), pelleted again and re-suspending in 80 µl RPMI+FBS. Twenty µl of magnetic bead labelled antiCD14 antibody was added for positive selection of monocytes and followed by incubation for 15 min at 4 °C. Cells suspension was then washed with 1 ml RPMI+FBS, pelleted by centrifugation at 700 x g 10 min (B9/A5) and re-suspended in 500 µl RPMI+FBS. Magnetic-activated cell sorting (MACS) columns were prepared by washing with 3 ml of RPMI+FBS while placed in the column of the MACS separator. Cell suspensions were added to the columns and immediately washed three times with 3 ml of RPMI+FBS. The cell suspension flow through was collected into sterile 15 ml flacon tubes. **Monocytes** were isolated by removing the column from the magnetic field of the MACS separator and eluted into a sterile 15 ml flacon with 5 ml of RPMI+FBS using a column plunger. **Lymphocytes** were isolated by pelleting the flow-through wash fraction at 300 x g for 10 min (B9/A5) and resuspension in 80 µL of RPMI+FBS. 20 µl each of magnetic beads labelled antiCD61 and anti235a antibodies were added to positively select out platelets and erythrocytes, followed by incubation for 15 min at 4 °C. Cells suspension was then washed with 1 ml RPMI+FBS, pelleted by centrifugation at 700 x g 10 min (B9/A5) and re-suspended in 500 µl RPMI+FBS. The cell suspension was added to the MACS column and immediately washed three times with 3 ml of RPMI+FBS. The cell suspension flow through was collected into sterile 15 ml falcon tubes. Cell fractions were then pelleted at 700 x g 10 min (B9/A5) and re-suspended in 1 ml warm sterile XF base media for counting using a haemocytometer.

## T lymphocytes (T cells)

Whole blood was collected into 6 x 9 mL EDTA tubes and diluted 1:1 with PBS. Diluted blood was layered onto 25 mL of 15 mL Ficoll in 4 x 50 mL falcon tubes. Tubes were spun at 1000 x g for 20 min (no acceleration or brake) in a swinging bucket centrifuge. PBMC layer was carefully removed into 2 x 50 mL falcon tubes, made up to 50 mL with RPMI+FBS and centrifuged at 500 x g for 5 min with brake. Pellets were re-suspended, combined and made up to 50 mL with RPMI+FBS. PBMS cells were counted by haemocytometer before cell solution was centrifuged at 300 x g (with brake) for 5 min and re-suspended in antibodies as follows: Target cell types (monocytes, B cells, NK cells) were calculated at 50% of total cells counted. Monoclonal antibodies (mAb) used were

produced in house from hybridomas obtained from American Type Culture Collection (ATCC). Fifty µL of each mAb were added per million target cells using OKMI (CD11b) for monocytes and L243 (HLA-DR) for monocytes, NK cells and B cells. Cell-mAb solution was placed on ice for 20 min then made up to 50 mL with RPMI+FBS and centrifuged at 350 x g for 5 min (with brake) and re-suspended in 250 µL RPMI+FBS. Ten µL per million targets of goat anti-mouse IgG microbeads were first washed with 2 mL RPMI+FBS in a magnetic field then added to cell mAb solution. Tubes were placed on ice for 30 min with regular agitation. Cell-mAb-microbead solution was made up to 2 mL with RPMI+FBS and supernatant was collected while tube was placed within a magnetic field. Collection was repeated with a further 2 mL of RPMI+FBS. The supernatant containing purified T cells was counted using a haemocytometer. T cell purity was measured using CD3-PE incubation (15 min) and flowcytometry. T cell solution was pelleted at 300 x g for 5 min (with brake) and re-suspended to the appropriate concentration with warm XF-DMEM media.

### 2.2.2 Seahorse Extracellular Flux (XF) Analysis

#### Preparation of XF24 Sensor Cartridge

On the day prior to the assay the XF24 sensor cartridge was hydrated by adding 1 ml of the XF calibrant solution to the utility plate and lowering the sensor cartridge to submerge the sensors. The cartridge was placed in a non-CO2 37 °C incubator overnight until required. **Modulator drugs were made up with sterile XF base media and loaded into cartridge injection ports immediately before the commencement of the XF assay.**

#### Preparing the XF- DMEM

XF assays require a non-buffered medium to accurately measure the extracellular acidification rate (ECAR). Two media types were used in assays (XF Base medium and XF Assay medium). Each was set to pH 7.35 ± 0.5, filter sterilised and kept warm in a 37 °C

water bath. XF base media was supplemented with 25 mM D-glucose, 1 mM pyruvate and 2 mM L- glutamine. XF assay media was supplemented with 25 mM D-glucose, 1 mM pyruvate and 4 mM L- glutamine.

### Plating of Cells

Cell-tak cell adhesive was freshly prepared to the recommended concentration for XF24 microplates of 2.4 µg/ml adjusted to pH 7.2-7.8 using 1M NaOH. 50 µl of the Cell-tak solution is applied to each well of the microplate and after 20 min was washed twice with 200 µl of PBS and aspiration. The plate was air dried for an additional 20 min then warmed to room temperature in the cell culture hood before seeding. One hundred µl of the desired cell suspension was seeded using a multipipettor pipette to the side of each of the 20 wells. Four additional wells remained unseeded to be used for background temperature and pH determination. The cell pate was centrifuged at 200 x g for 1 sec with no brake, rotated 180° and centrifuged again at 300 x g for 30 sec (no brake). Cells were incubated (not supplemented with $CO_2$) for 30 min at 37°C before being topped up with 500 µL of warm XF base media (at the top-side of the well wall) and further incubated for 15-25 min. Cells were observed under a microscope before being placed in the XF analyser.

## 2.2.3 XF Assay Protocol

The XF assay protocol was set to measure the change in dissolved $O_2$ concentration from within a fixed 7µl volume of extracellular media over a four minute time period. The resulting metric is the oxygen consumption rate (OCR) which is given as is an indicator of mitochondrial respiration and is expressed as picomols per minute (pmol/min). Absolute OCR measurements are recorded at 8 minute intervals. Each begins with 2 minutes of agitation to allow the extracellular media to mix, followed by 2 minutes of waiting time and 4 minutes of measurement upon the formation of the transient fixed volume micro-chamber, giving a mix/wait/measure setting of 2/2/4 min. Each drug injection is followed by two subsequent OCR measurements. Five consecutive

measurement points were made to establish a steady basal respiration period before the first drug oligomycin (0.75 μM) was injected into the extracellular media to inhibit ATP synthase. FCCP (variable) was then injected to uncouple the proton gradient across the inner mitochondrial membrane, and antimycin A (10 μM) was added to inhibit complex 3 and consequently the ETC.

The individual bioenergetics parameters of OXPHOS as illustrated in Figure 1.4 were calculated as follows: **Non-mitochondrial respiration** = minimum rate measured after injection of Antimycin A. **Basal** respiration = (last rate measured before Oligomycin injection) – (non-mitochondrial respiration rate). **Maximal respiration** = (maximal rate measured after FCCP injection) – (non-mitochondrial respiration rate). **ATP production** = (last rate measured before Oligomycin injection) – (minimum rate measured after Oligomycin injection). **Proton leak** = (minimum rate measured after Oligomycin injection) - (non-mitochondrial respiration rate). **Spare reserve capacity** = (maximal respiration – basal respiration).

### 2.2.4 Protein Assay

The XF media was carefully aspirated from each well. 20 μl of lysis buffer was added to each well, mixed with pipette and allowed to sit for 5 mins (RT). 2 μl of cell lysate was added to the Direct Detect® infrared spectrometer assay cards which were dried at 37°C for 10 min before protein content was quantified.

# Chapter Three: Results

## 3.1 Platelets

Platelets were isolated and purified by differential centrifugation as described in Section 2.2.1. Typically, 4 x 9 ml EDTA tubes were used to isolate ~1-2 x $10^9$ platelets, providing enough cells to seed all 20 available wells at the initial seeding density of 50 x $10^6$ platelets per well. Prostacyclin ($PGI_2$) was used to inhibit platelet aggregation during pellet re-suspension. $PGI_2$ acts by antagonizing thromboxane A2 and stimulating platelet adenylyl cyclase (55). It was found necessary to make up $PGI_2$ in sterile $H_2O$ at a pH of 11 and store single use aliquots in a -80 °C freezer. Platelets responded best to pelleting and re-suspension after at least 30 minutes' rest following the initial whole blood PRP spin. Cell Tak and plate centrifugation was found to successfully adhere platelets to the well floor for the duration of the 88 minute assay. Density experiments found that under the microscope platelets appear confluent at 50 x $10^6$ cell per well (Figure 3.1).

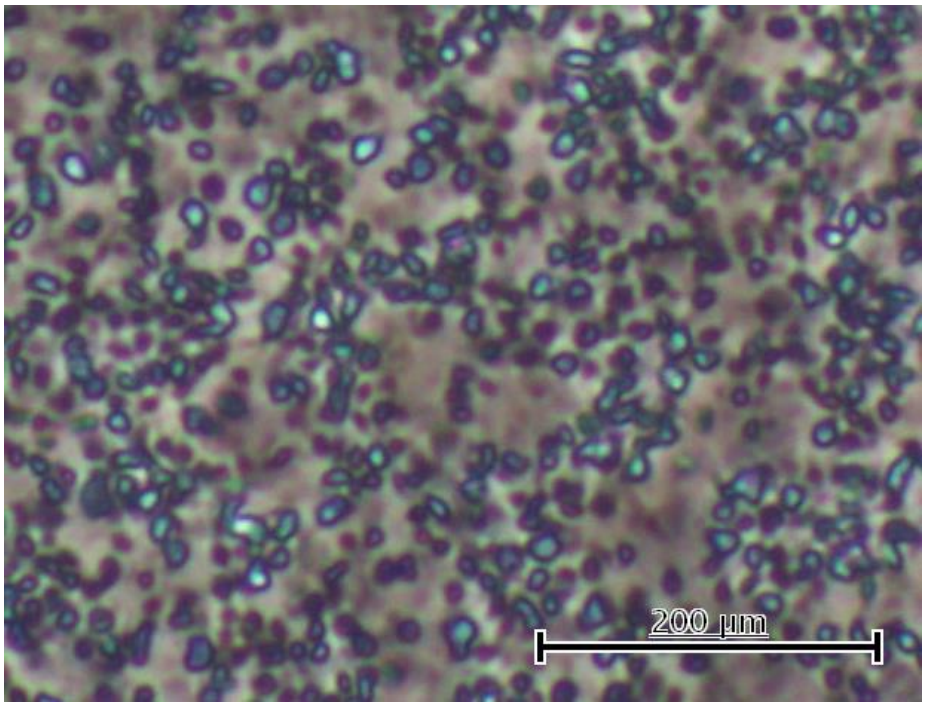


***Figure 3.1 Platelets adhered to XF24 well plate.*** *Confluency was observed at 50 x 106 platelets per well.*

### 3.1.1 Mitochondrial Stress Test

Oxygen consumption rate was calculated at every measurement point for each of the 20 wells of the XF24 plate used in the mitochondrial stress test. Every well produced its own individual bioenergetic trace (Figure 3.2), which, combined, give a mean value for each technical replicate within a group. A representative mean bioenergetic trace from a mitochondrial stress test is shown in Figure 3.3. Basal respiration was stable before the addition of modulating drugs, which once injected into the extracellular media were able to successfully isolate the desired components of OXPHOS as expected.

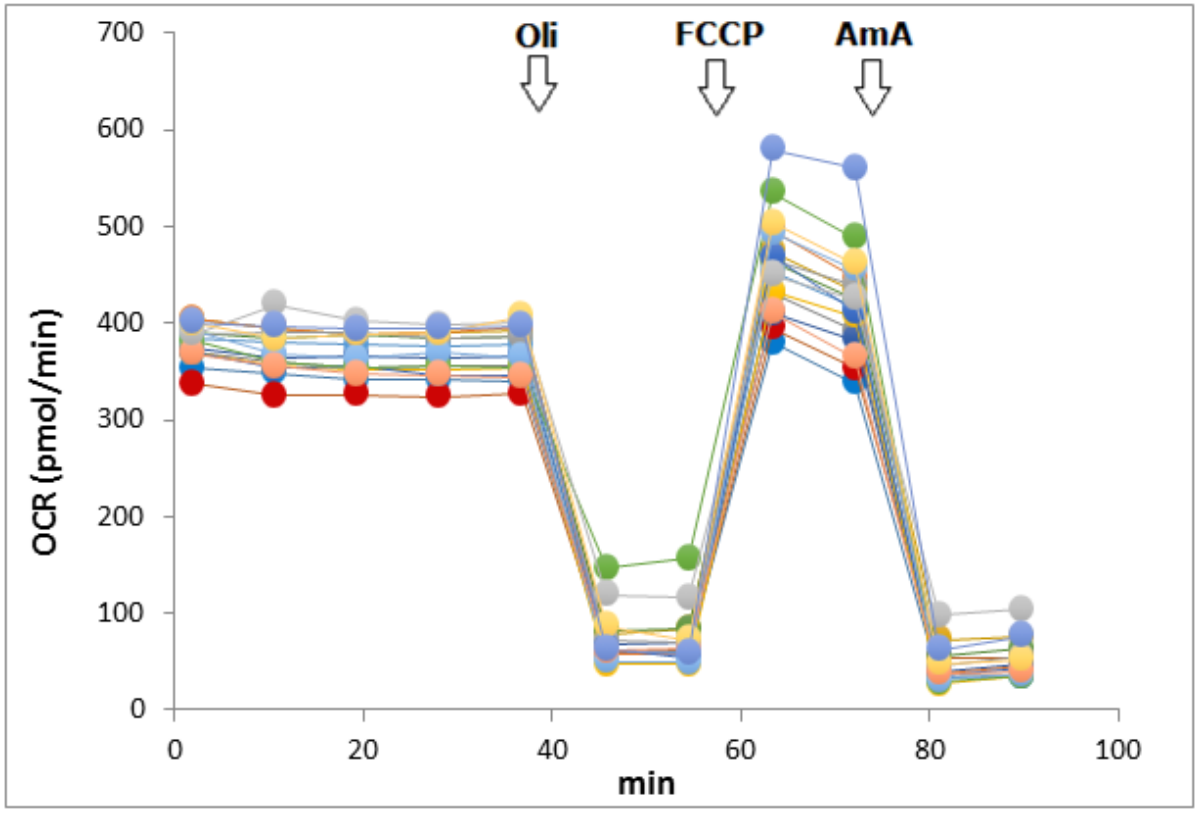


***Figure 3.2. Individual bioenergetics traces from a mitochondrial stress test.*** *Plate K, 40 x $10^6$ platelets per well, FCCP = 0.6µM. Data represent individual values from 17 wells.*

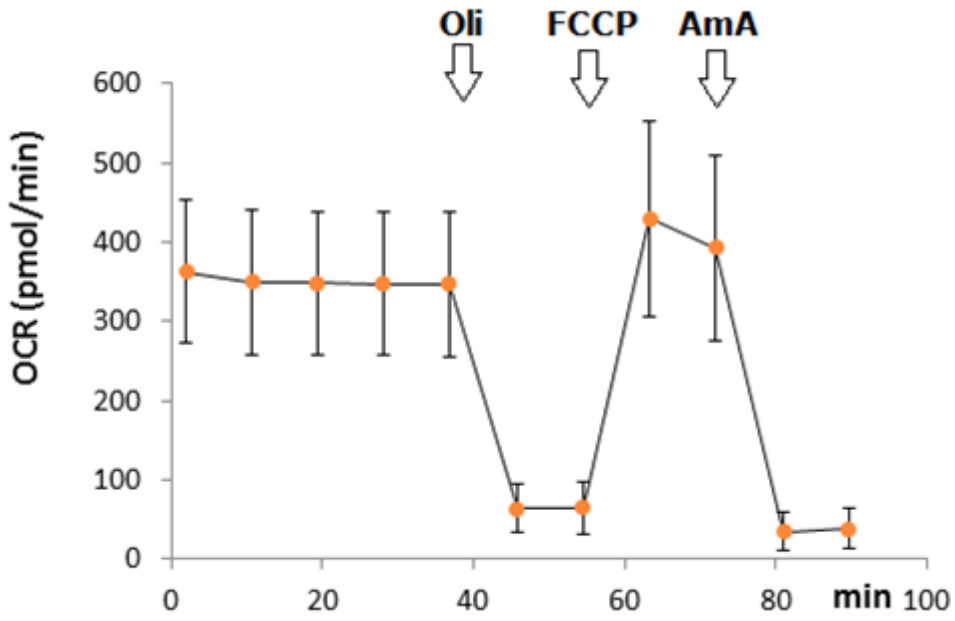


***Figure 3.3. Representative mean bioenergetics trace from a mitochondrial stress test.*** *3 Plate K, 40 x $10^6$ platelets per well, FCCP = 0.6µM. Data represent mean values from 17 wells ± standard deviation.*

During the same measurement periods the change in proton concentration was also measured against time to determine the extra-cellular acidification rate (ECAR), which is predominantly a measure of lactic acid formed during glycolytic energy metabolism (Figure 3.4). For the same experiment, a low and stable ECAR value was observed during the basal measurement period. Upon the introduction of oligomycin a rapid increase in ECAR was observed, which is reflective of increased glycolytic metabolism due to the inhibition of ATP synthase.

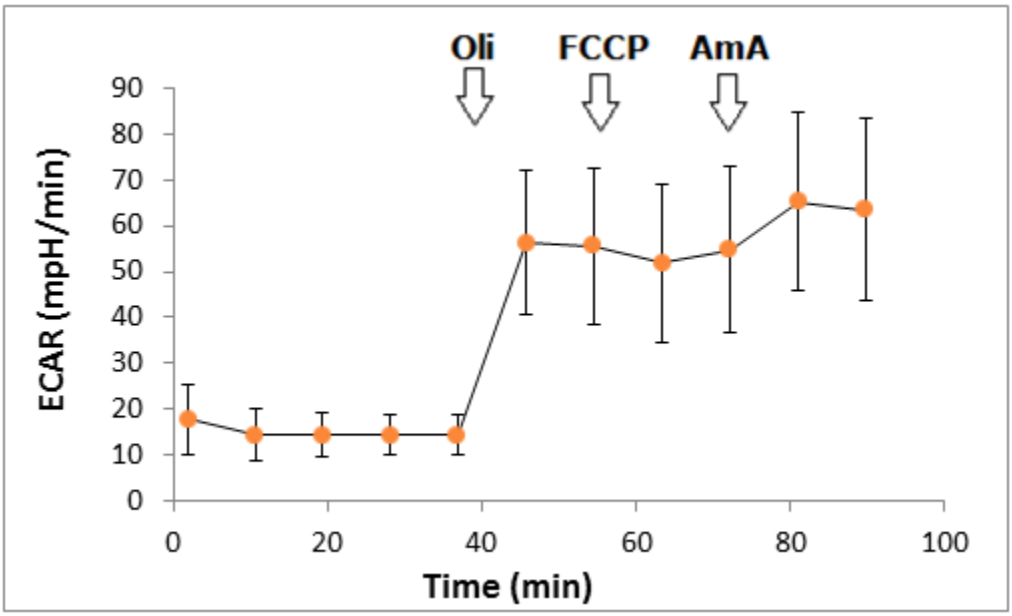


***Figure 3.4 Representative platelet ECAR trace from a mitochondrial stress test.*** *Plate K, 40 x $10^6$ platelets per well, FCCP = 0.6µM. Data represent mean values from 17 wells ± standard deviation.*

The individual OXPHOS bioenergetic parameters of the same representative experiment are given in the bar graph in Figure 3.5. OCR is given here as absolute values before normalisation.

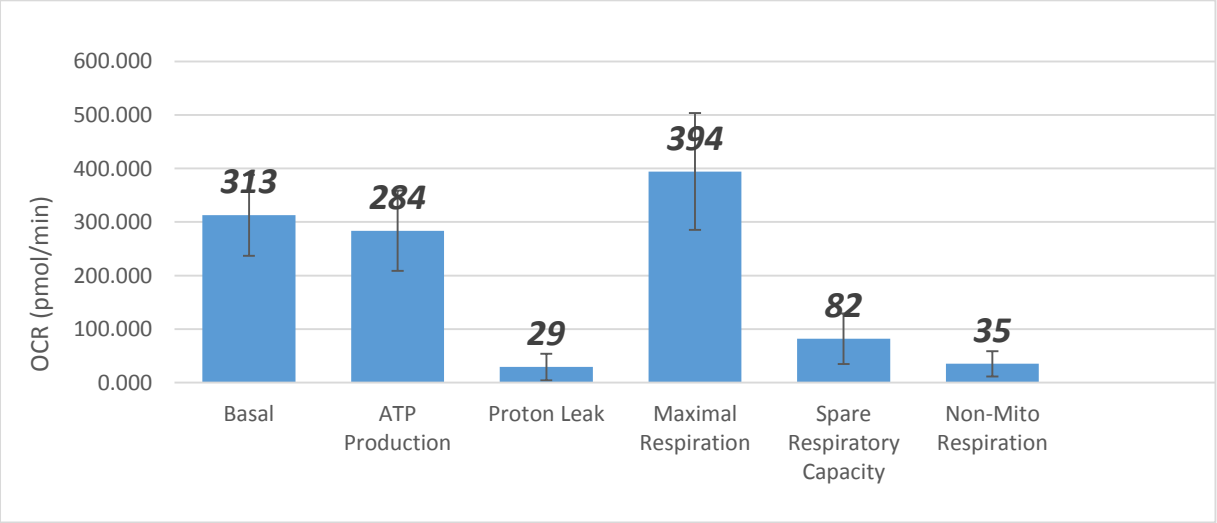


***Figure 3.5 Bioenergetics parameters of OXPHOS - platelets.*** *Plate K. Data represent mean values from 17 wells ± standard deviation.*

The same bioenergetic parameters can be represented as a percentage of basal respiration, as shown in Figure 3.6. This has the effect of normalising the parameters relative to basal respiration, and counteracting any variation in cell seeding number that may occur between experiments.

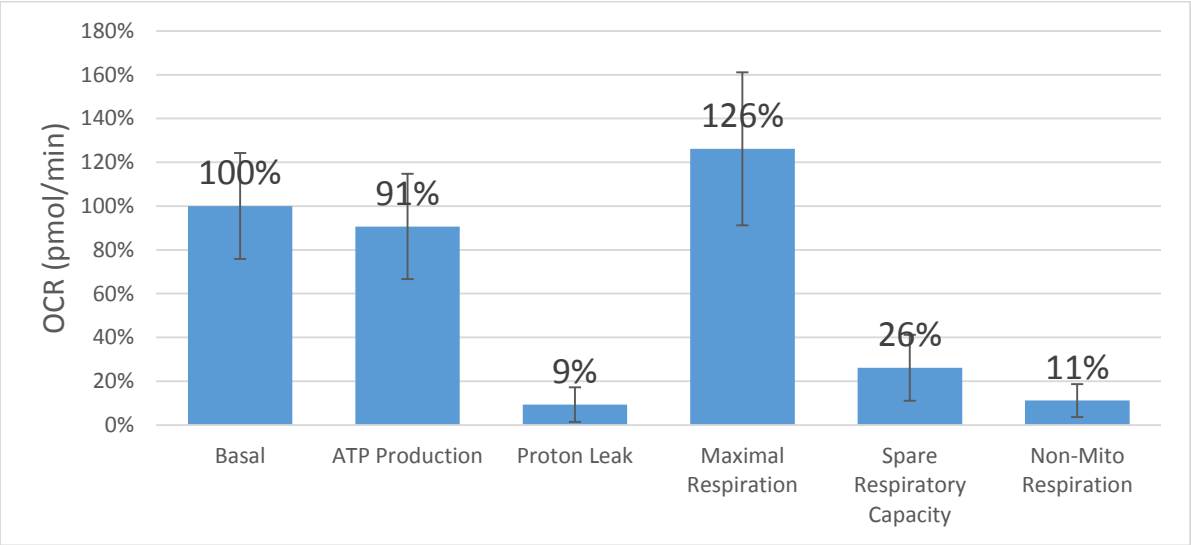


***Figure 3.6 Bioenergetics parameters of OXPHOS as a percentage of basal respiration - platelets.*** *Plate K, 40 x 106 platelets per well, FCCP = 0.6µM. Data represent mean values from 17 wells ± standard deviation.*

Four of the bioenergetic parameters are represented in the single index termed the bioenergetic health index (BHI) (Figure 1.5) as developed by Dr. Victor Darley-Usmar at the University of Alabama at Birmingham. For this basic derivation the exponents for each parameter of the equation are set to one. The BHI for the same representative experiment is shown in Figure 3.7. Individual BHI values are calculated for each well and then averaged to provide the mean BHI for that group. One additional well has been omitted due to having a negative value for one of the four biometric parameters.

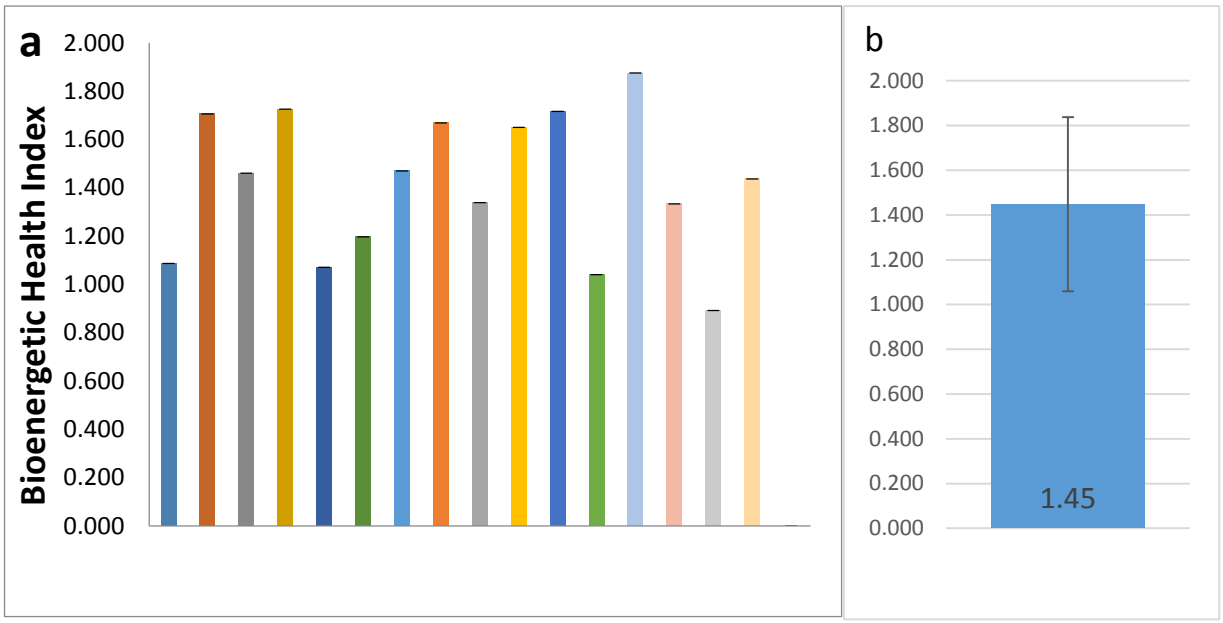


***Figure 3.7 BHI for platelets – plate K.*** *A single metric encompassing four bioenergetic parameters measured by the mitochondrial stress test. (a) BHI calculated from each individual well; (b) is a mean value, n=16 ± standard deviation.*

### 3.1.2 Abnormal Results

12 platelet mitochondrial stress tests assays were conducted using blood donated from 10 individuals (6 female, 4 males) ranging from 21 to 56 years of age. These preliminary experiments were carried out to optimize important aspects of the stress test assay such as cell seeding density, FCCP concentration and glutamine media supplementation. Each assay involved seeding 20 available wells - of the XF24 plate - with platelets belonging to a single healthy donor. Groups of 4 or 5 technical replicates were allocated to each variable being examined, while the other assay parameters stayed uniform. To varying degrees each experiment contained wells with abnormal results, with OCR or ECAR measurements differing from the characteristic response reported in Figures 3.3 and 3.4. The abnormal wells were consequently omitted from normal results data. There appeared to be four different types of abnormal response which were categorised by the following criteria:

(1) Well displayed a metabolic switch to glycolysis, shown by a high or increasing ECAR during the basal measurement period and a declining or erratic OCR.

(2) OCR showed a normal pattern, but the absolute value fell outside two standard deviations of the mean of that group.

(3) OCR was comparatively unresponsive or showed uncharacteristic response to modulators.

(4) Well failed to establish a stable basal OCR during the basal measurement period.

A representative illustration of each criterion is shown in Figure 3.8, and a schematic of each 24 well plate used in the 12 experiments is shown in Figure 3.9. In the latter figure, each abnormal well is assigned a number (as above) to categorise their omission criteria. A supplementary table is included (Table 3.1) to detail each experiment type and list the experimental parameter being optimised. In this table the total number of abnormal wells is listed along with the frequency of each of the four classification criteria. The abnormal wells are further colour coded to aid in visualising patterns and frequencies. The number of abnormal wells varied significantly between individual experiments.

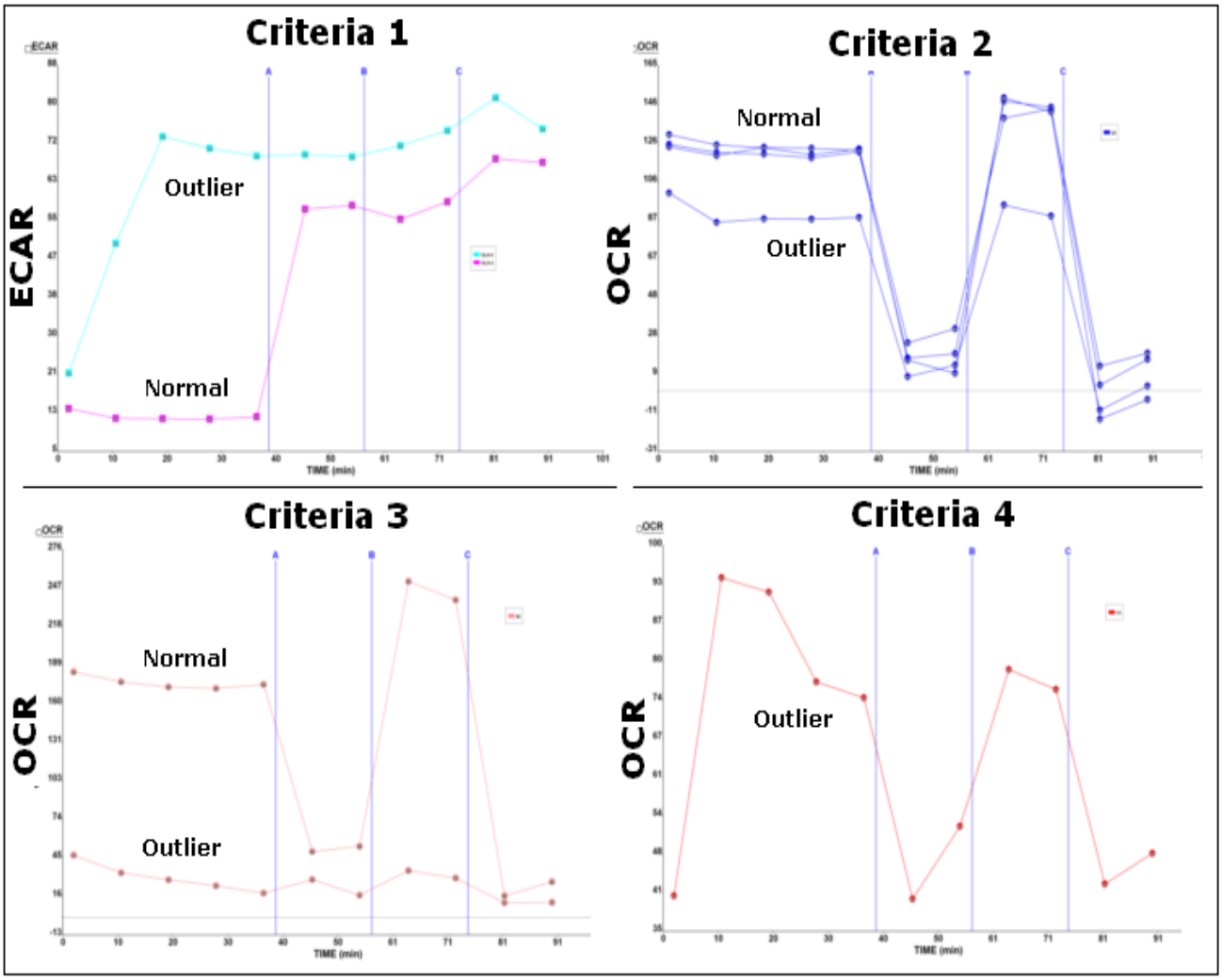


***Figure 3.8 Demonstrative traces of the four criteria used to categorise abnormal results.*** *Bioenergetic traces are given to illustrate the pattern seen in each qualifying criterion.*

Experiments from plates G, H and L have half or more wells being omitted. Others such as plates B, J and K show relatively small occurrences. Five plates (C, F, G, H, and L) have the highest frequency of outliers which fall under criterion 1, while four plates (A, B, E, and K) have no occurrences.

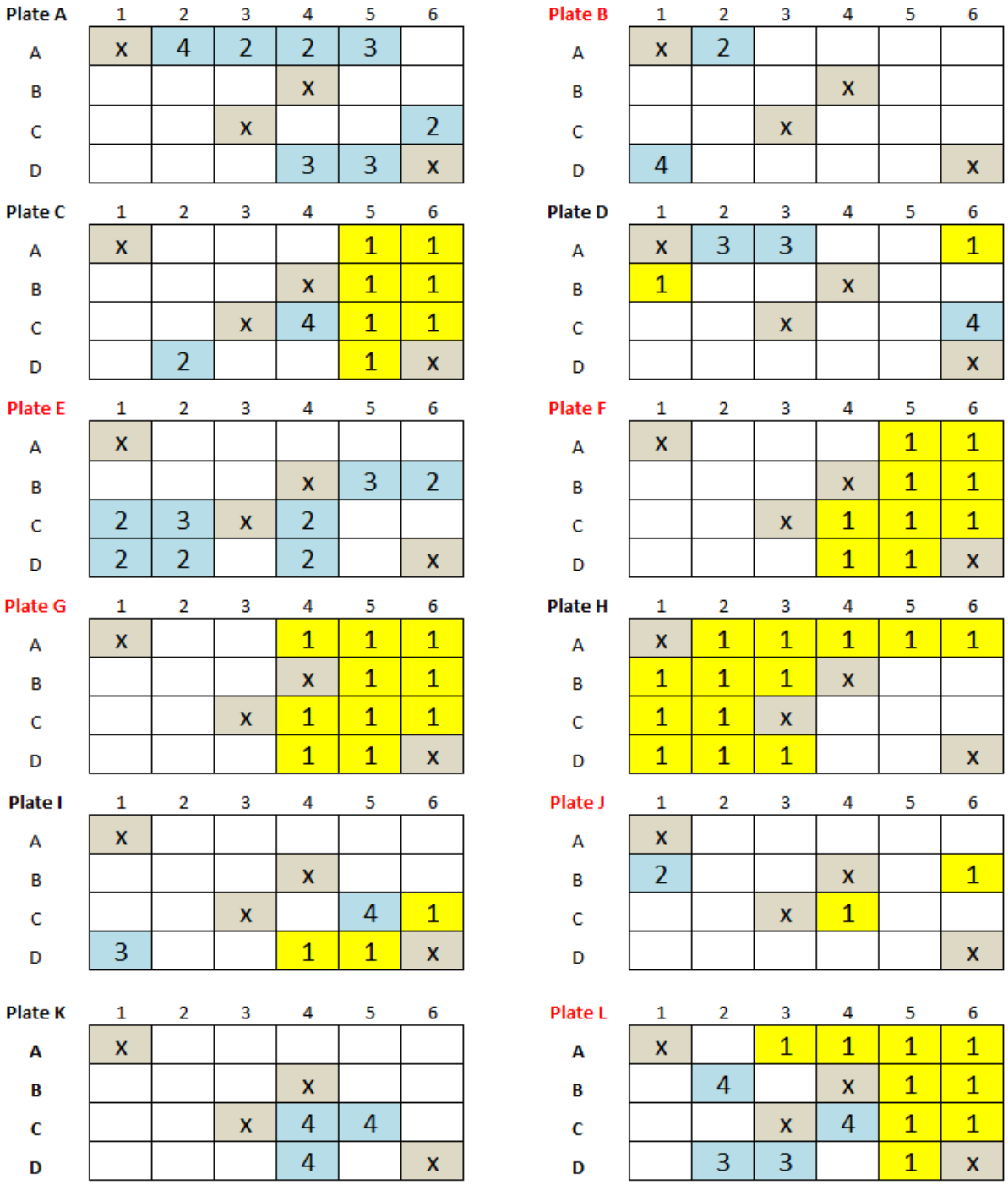


***Figure 3.9 Schematic of each of 24 well cell-plates used in 12 optimisation experiments****. Each numbered square represents an abnormal well excluded from results data. Squares marked with 'x' represent background wells.*

***Table 3.1. Record of twelve platelet optimisation experiments.***

| Plate | Donor | Date | Optimisation experiment | Replicates | Oli (μM) | FCCP (μM) | AMA (μM) | Seeding density | Gln total (mM) | Abnormal wells | 1 | 2 | 3 | 4 |
|---|---|---|---|---|---|---|---|---|---|---|---|---|---|---|
| A | A01 | 4-Jun | Platelet seeding 1 | 20 | 0.75 | 0.6 | 10 | varied | 6 | **7** | | 3 | 3 | 1 |
| B | A06 | 17-Jun | Platelet seeding 2 | 20 | 0.75 | 0.6 | 10 | varied | 6 | **2** | | 1 | | 1 |
| C | A07 | 23-Jun | Platelet seeding 3 | 20 | 0.75 | 0.6 | 10 | varied | 4 | **9** | 7 | 1 | | 1 |
| D | A01 | 24-Apr | FCCP Variation 1 | 20 | 0.75 | varied | 10 | 70m | 4 | **5** | 2 | | 2 | 1 |
| E | A04 | 24-Jun | FCCP Variation 2 | 20 | 0.75 | varied | 10 | 40m | 4 | **8** | | 6 | 2 | |
| F | A08 | 30-Jun | FCCP Variation 3 | 20 | 0.75 | varied | 10 | 40m | 4 | **9** | 9 | | | |
| G | A09 | 3-Jul | FCCP Variation 4 | 20 | 0.75 | varied | 10 | 40m | 4 | **10** | 10 | | | |
| H | A02 | 10-Jun | Glutamine Variation 1 | 20 | 0.75 | 0.6 | 10 | 40m | varied | **13** | 13 | | | |
| I | A05 | 12-Jun | Glutamine Variation 2 | 20 | 0.75 | 0.6 | 10 | 40m | varied | **5** | 3 | | 1 | 1 |
| J | A03 | 16-Jun | Glutamine Variation 3 | 20 | 0.75 | 0.6 | 10 | 40m | varied | **3** | 2 | 1 | | |
| K | A10 | 3-Aug | Glutamine Variation 4 | 20 | 0.75 | 0.6 | 10 | 40m | varied | **3** | | | | 3 |
| L | A02 | 3-Aug | FCCP Variations 5 | 20 | 0.75 | varied | 10 | 40m | 4 | **13** | 9 | | 2 | 2 |

### 3.1.3 Metabolic Switch to Glycolysis

Criterion 1 wells have displayed a metabolic switch to glycolysis as shown by a high or increasing ECAR during the basal period and a declining or erratic OCR. These contrasting bioenergetic traces are illustrated in Figure 3.10, which shows OCR and ECAR traces for normal and abnormal wells (plate G). OCR begins near normal levels for the first measurement point and then quickly declines over the next few measurement points to sit at approximately the level of non-mitochondrial respiration. By contrast, ECAR values usually start around low levels and rapidly increase over the following two measurements. The metabolic switch appears to occur during the early stages of the stress test assay but before the introduction of any modulators.

Criterion 1 is the dominant form of abnormality, occurring most frequently (8/12 experiments, 55/240 wells). In plates where criterion 1 is dominant, the affected wells appear grouped to a particular side of the well plate instead of being randomly distributed throughout, despite cells being seeded in a random sequence or by row using a multipipette. This abnormality occurs irrespective of the variable being optimised as it is evident in each of the three types of optimisation experiment being performed (as detailed in Table 3.1).

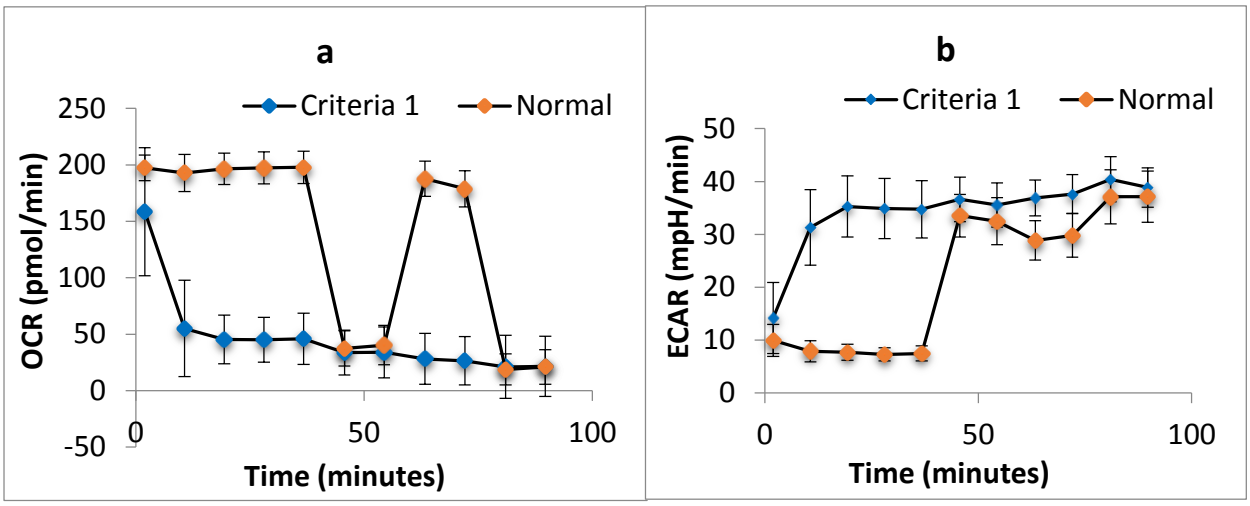


***Figure 3.10 OCR and ECAR bioenergetic traces (plate G).*** *Figures show two groups of either normal or abnormal wells (n=10 for each group). (a) Mitochondrial stress test profile representing bioenergetics components of OXPHOS. (b) ECAR which represents GL.*

Inspection of the wells at the conclusion of the experiment revealed platelets from criterion 1 were aggregating to varying degrees, as illustrated in Figure 3.11. This aggregation occurs during the course of the experiment, as the cells begin the procedure in a confluent monolayer but finish in varying clustered formations.

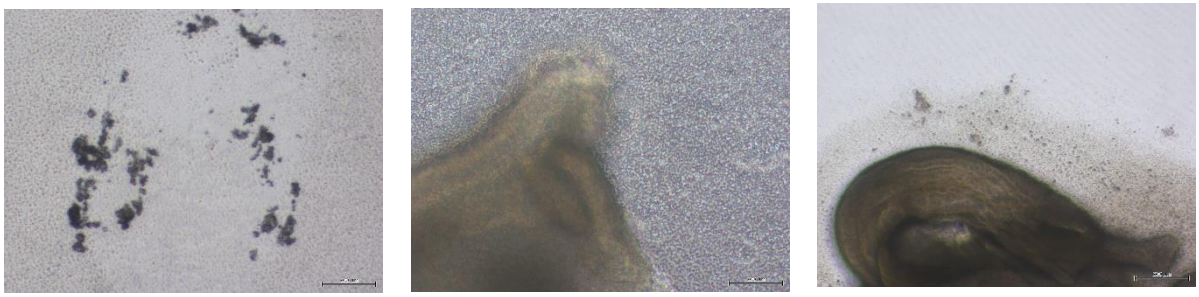

***Figure 3.11 Representative microscope photos at the conclusion of the mitochondrial stress test assay.*** *Images show varying degrees of platelet aggregation from small clumps to large clumps to total aggregation (left to right). Photos from the same assay.*

To ascertain whether the pH of the extracellular media might be causing a metabolic switch, the background wells of two glutamine (GLN) optimization experiments were examined (Figure 3.12). Unbuffered XF-DMEM media used in these experiments was initially set to a pH of 7.35 at a temperature of 37 °C. Both experiments shown are exact replicates which differ only by blood donor. The top charts display pH and OCR values from the four background wells during the course of the experiment. Figure 3.12 highlights the similarities in both pH and OCR of the background wells. Background pH for each experiment starts at around 6.9 and increases during subsequent measurements to level out at a range of 7.0 to 7.1. OCR traces show a similar increase over the time points of these experiments. While both experiments have similar background pH and OCR they have drastically different result outcomes, as shown in the schematic of the well plate below each graph. Plate H has 13 abnormal wells categorised as criterion 1, while plate J has just 3 abnormal wells. The contrasting outcomes of these experiments appears independent of glutamine supplementation and pH conditions of the media used.

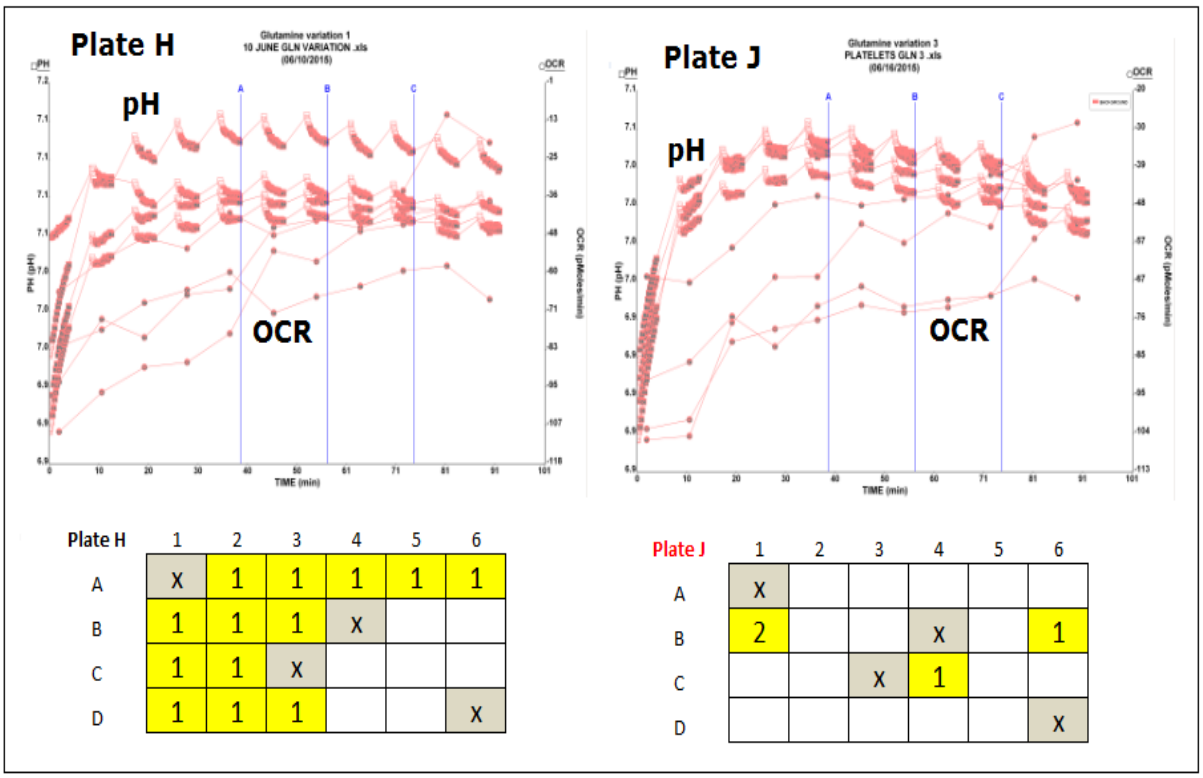


***Figure 3.12 Comparison of background wells from two glutamine optimization experiments (H and J).*** *Top graphs show pH and OCR measurements of the background wells from each experiment. The bottom schematic illustrates abnormal wells from the corresponding experiments above.*

### 3.1.3 Optimisation Results

Despite the high occurrence of abnormal wells, it was possible to use the data obtained from the normal profiles. The loss of data that resulted from having to exclude abnormal or 'outlier' wells made comparison of valuations difficult. Figure 3.13 illustrates this difficulty. Four experiments from four different blood donors are compared in this bar graph. The number of replicate wells used in calculating the mean values is listed at the base of each column. Each group in all experiments had 5 wells allocated to each variable, but due to the exclusion of abnormal wells the replicates vary from 1 to 5 wells.

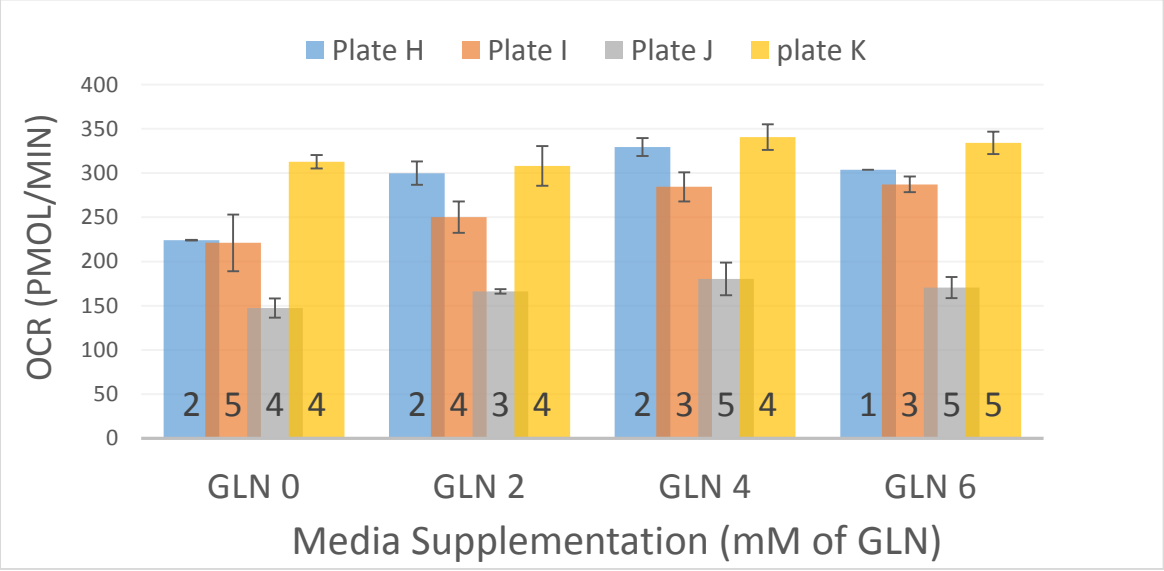


***Figure 3.13 Glutamine optimisation experiments – basal respiration.*** *Platelets from four donors were assayed under varying concentrations of glutamine-supplemented media. Technical replicates are numbered at the base of each column. 40 x $10^6$ platelets per well, FCCP = 0.6µM. Data represent mean absolute values ± standard deviation.*

The same data set is represented in Figure 3.14. Here each measurement is given as a percentage of the data set labelled GLN 0, which had no additional glutamine added to the XF media (XF assay media already contains 2 mM glutamine). Plate H appears most responsive to glutamine supplementation, but the low number of replicates used in these averages is unsatisfactory. Plate K had the lowest number of wells omitted and appears

comparatively unresponsive to increasing concentration of glutamine. Plates I and J show a positive response to increasing glutamine supplementation.

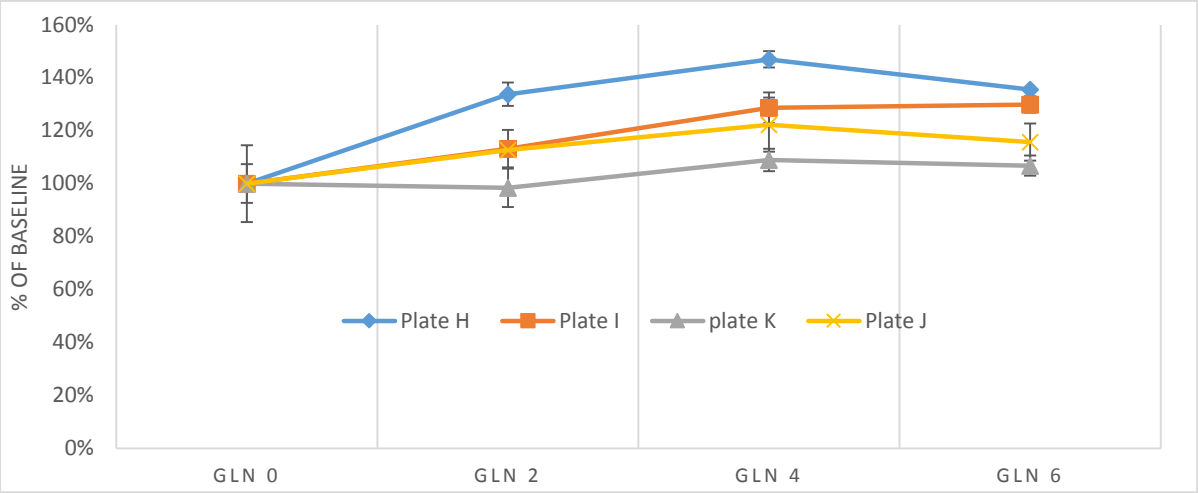


***Figure 3.14 Glutamine optimisation experiments - % change basal.*** *Platelets from four donors were assayed under varying concentrations of glutamine-supplemented media. Measurements given as percentage change from a baseline point designated as GLN 0. Data represent mean values ± standard deviation.*

The impact of glutamine supplementation on platelet reserve capacity is also shown in Figure 3.15. In this graph, spare respiratory capacity is given as a percentage of basal respiration. Plate H again is most responsive to increased glutamine concentrations with supplementation of 2 mM (4 mM total) achieving the maximal effect. All further platelet experiments were carried out with 2 mM glutamine supplementation to bring the glutamine concentration to 4 mM and in-line with current literature.

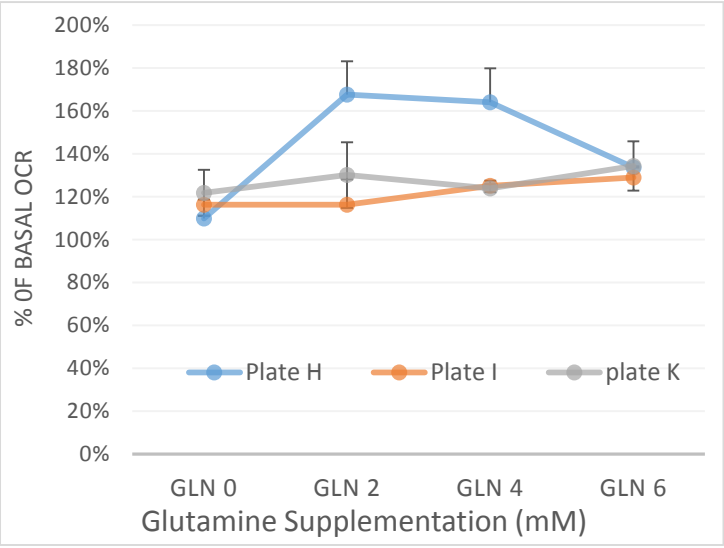


***Figure 3.15 Glutamine optimisation experiments – spare capacity %.*** *Measurements given as percentage change of basal respiration. Data represent mean values ± standard deviation.*

Platelet seeding density assays were also conducted to optimise the number of platelets seeded into each well of the XF24 cell microplates (Figure 3.16). The seeding density of 40 million platelets per well was chosen for three reasons: 1 - cells visually appear confluent under microscope; 2 – OCR values lie on the linear response region in each of the three optimisation experiments; 3 - OCR values of at least 200 pmol/min are optimal for the instrument's sensitivity. At higher densities (80 x $10^6$ per well) a drop in OCR values was seen in plates A and C.

As shown in Table 3.1, no consistent adverse effects were seen as a result of over-confluent platelet seeding. Two of the three platelet seeding experiments produced results with no abnormal wells from criterion 1. In one experiment (plate C), 7 wells displayed a metabolic switch to glycolysis, but there was no discernible pattern in relation to seeding density, as wells from all densities were affected.

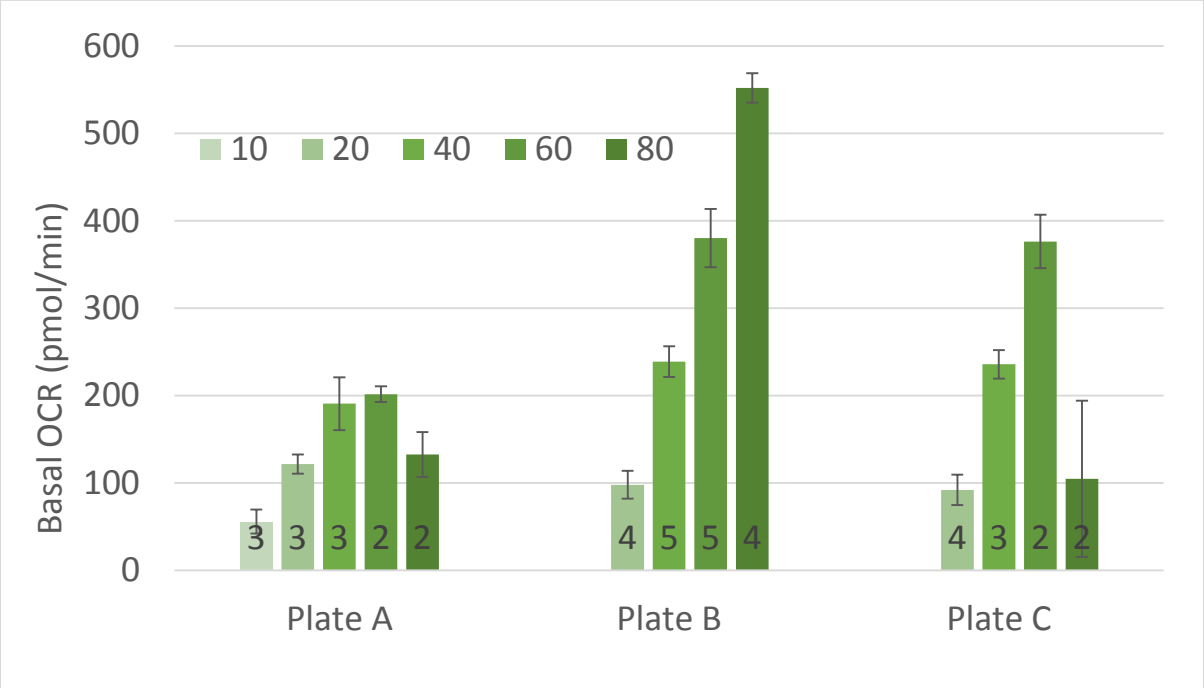


***Figure 3.16 Platelet seeding density experiments.*** *Platelets from three donors were assayed under varying platelet densities of 10-80 x $10^6$ cells per well. Technical replicates are numbered at the base of each column. Data represent mean values ± standard deviation.*

Other biometric parameters were examined to see if they were affected by seeding density. Similar declines in line with basal respiration were seen at higher seeding densities. The density of 40 x $10^6$ platelets per well appears to show a positive OCR response in each of the parameters; however, the same problem with irregular technical replicate numbers meant interpretations of this data is difficult.

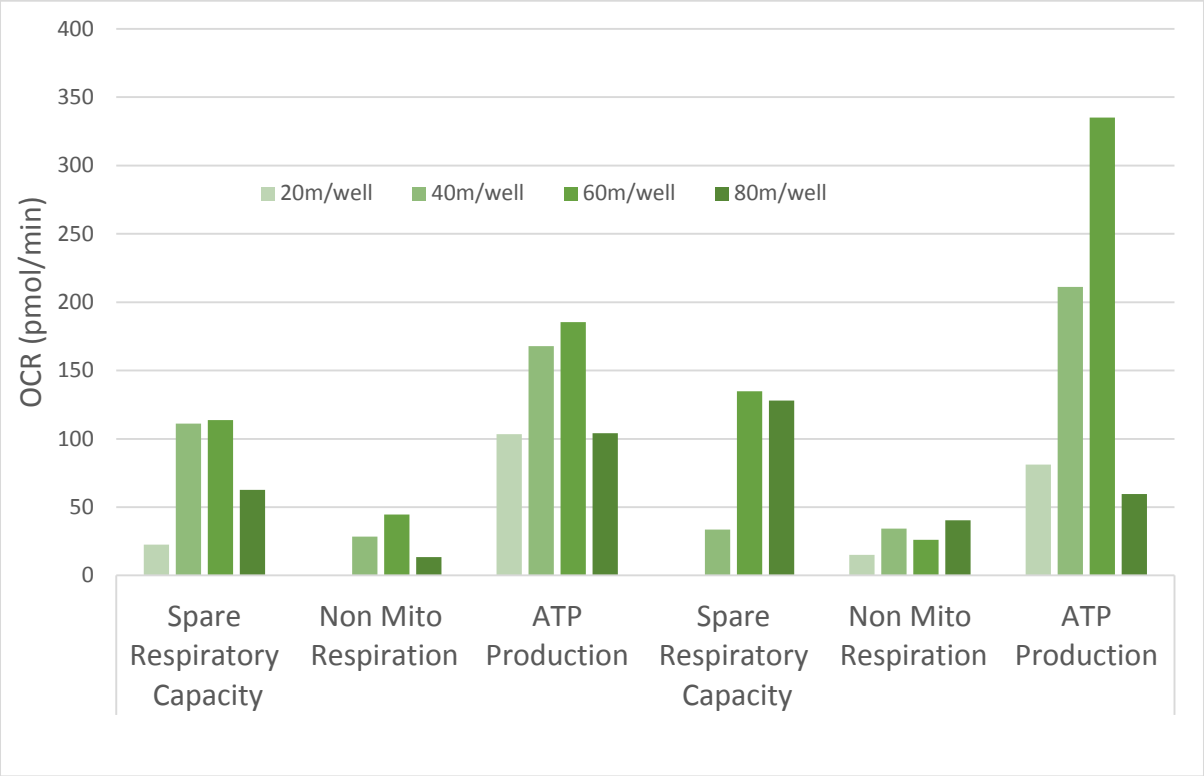


***Figure 3.17 Platelet biometric parameters from seeding density experiments.*** *Platelets from three donors were assayed under varying platelet densities. Technical replicates are numbered at the base of each column. FCCP = 0.6μM. Data represent mean values.*

FCCP experiments were also conducted to optimise the use of this cytotoxic ionophore. By shuttling protons across the inner mitochondrial membrane, this proton carrier collapses the proton gradient and prevents the usual PMF. This allows the ETC complexes to operate at their maximal rate and allows measurement of both maximal and spare reserve capacity. Titrating this drug is essential to both achieving the maximal spare reserve capacity and minimising the cytotoxic effects on the other cellular components for the remaining duration of the XF assay. Four FCCP optimisation experiments were carried out to determine the lowest FCCP concentration able to achieve the maximal uncoupling effect as represented by spare reserve capacity. Only one of these experiments produced interpretable data (Figure 3.18). The data set of 0.5 µM had three wells omitted as abnormalities, leaving only two remaining wells to record a mean value. The other three experiments had too many wells omitted due to abnormalities. Such inconsistencies within experiments hindered useful interpretation or comparison. It was not possible to reproduce results consistently due to the loss of data from abnormal wells, and so the use of 0.6 µM of FCCP was continued for all experiments, following the protocol of previous research (53).

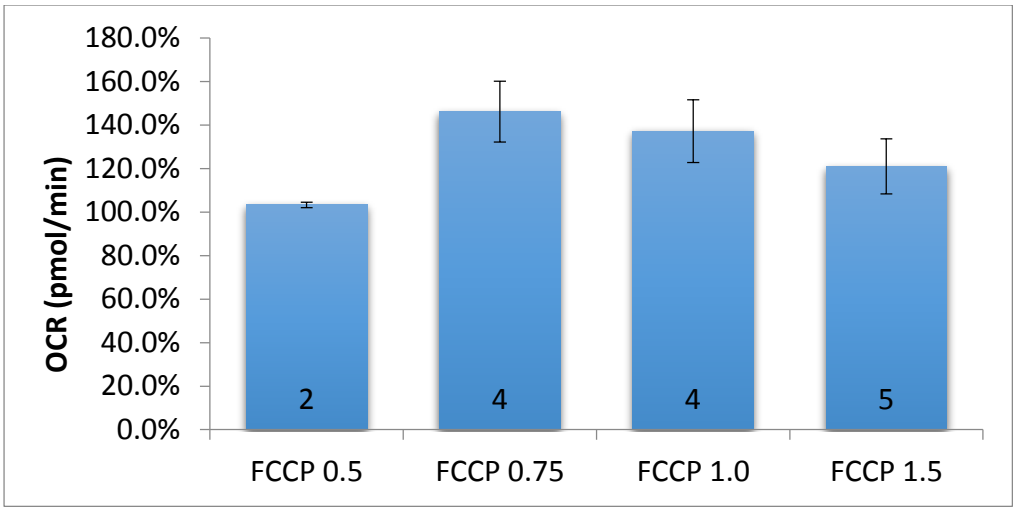


***Figure 3.18 Platelet FCCP optimisation experiment - Spare Respiratory Capacity (%)*** *Platelets (plate D) were assayed under varying FCCP concentrations (mM). Technical replicates are numbered at the base of each column. Oli = 0.75 µM, Ama = 10 µM. Data represent mean values ± standard deviation.*

### 3.1.4 Preliminary Results

Table 3.2 gives BHI calculations from the 7 experiments where this calculation could be made. Age, date and donor have also been included. Two of these values (D and F) have used a FCCP concentration that differs from the remainder. This data set is given to illustrate the concept of calculating BHI for donors of different ages; however, the experimental conditions are too irregular to enable comparison. This irregularity is due to the combination of having variations in experimental parameters and the resulting data loss from excluded wells. As detailed earlier, optimisation experiments required dividing the 20 available wells into groups of 5 replicates. For some experiments this resulted in very few normal replicates from which to make the necessary calculations. This is a problem that should easily be solved once optimisation experiments give way to normal data collection and 10 wells per donor can be used (n=10).

To calculate BHI a normal trace is required where all biometric parameters are successfully measured. A negative value for any of the parameters that constitute the BHI results in that well being excluded from BHI calculations. Hence further data loss was experienced when proton leak or non-mitochondrial respiration occasionally measured as a negative OCR value

***Table 3.2. Record of BHI from seven platelet optimisation experiments.***

| Plate | Donor | Date | Age | FCCP (µM) | BHI |
|---|---|---|---|---|---|
| A | A01 | 4-Jun | 21 | 0.6 | 1.56 |
| C | A07 | 23-Jun | 43 | 0.6 | 1.14 |
| D | A01 | 24-Apr | 21 | 1 | 1.4 |
| F | A08 | 30-Jun | 45 | 1.5 | 0.98 |
| H | A02 | 10-Jun | 33 | 0.6 | 1.91 |
| I | A05 | 12-Jun | 56 | 0.6 | 1.89 |
| K | A10 | 3-Aug | 31 | 0.6 | 1.4 |

## 3.2 Peripheral Blood Mononuclear Cells (PBMCs)

### 3.2.1 Monocytes and Lymphocytes

The protocol initially followed was designed to isolate and purify each of the three desired cell types (platelets, monocytes and lymphocytes) from the same blood sample (53). Whole blood was centrifuged and the platelet rich plasma was removed as per the platelet preparation protocol (chapter 2.2.1). The residual blood was then processed according to the monocyte and lymphocyte protocol using MACS separation. The resulting monocyte and lymphocyte preparations contained a high level of neutrophil contamination. Furthermore, the monocyte isolations also contained lymphocyte contamination as confirmed by flow cytometry (Figure 3.19). Further rounds of MACS separation purified the target cell but resulted in a yield too low for XF analysis. After using flow cytometry to test the Ficoll layers it was discovered that neutrophils were present at all density layers. This phenomenon was observed only when the whole blood had undergone the initial centrifugation for platelet isolation from PRP. It was decided from this point that the platelet centrifugation step was causing neutrophil contamination and should be discontinued. From this point dilute whole blood was overlaid onto Ficoll and platelets were prepared from separate blood samples.

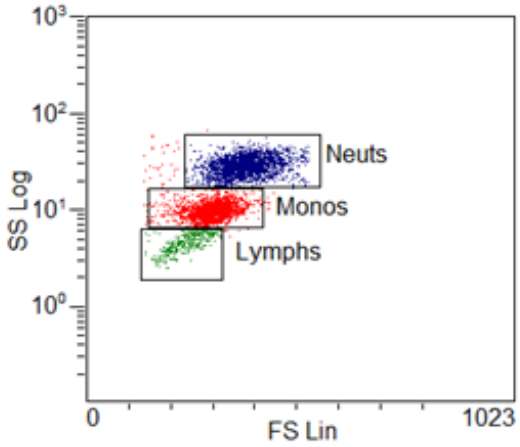


***Figure 3.19 Representative flow cytometry result from a monocyte preparation using MACS separation.*** *Lymphocytes 7%, Monocytes 46%, Neutrophils 46%.*

### 3.2.1 T Lymphocytes (T-cells)

Lymphocytes can be divided into three cell types: T cells, B cells and natural killer (NK) cells. T cells were isolated using negative selection to remove target cells (monocytes, B cells, NK cells) from a PMBC density isolation. On average, 20-35 x $10^6$ T cells were purified from 6 x 9 ml of whole blood, providing ample cells to seed 20 wells of a XF24 plate.

## Optimisation Results

The mitochondrial stress test analysis was conducted on varying T cell concentrations to determine the optimal seeding density (Figure 3.20).

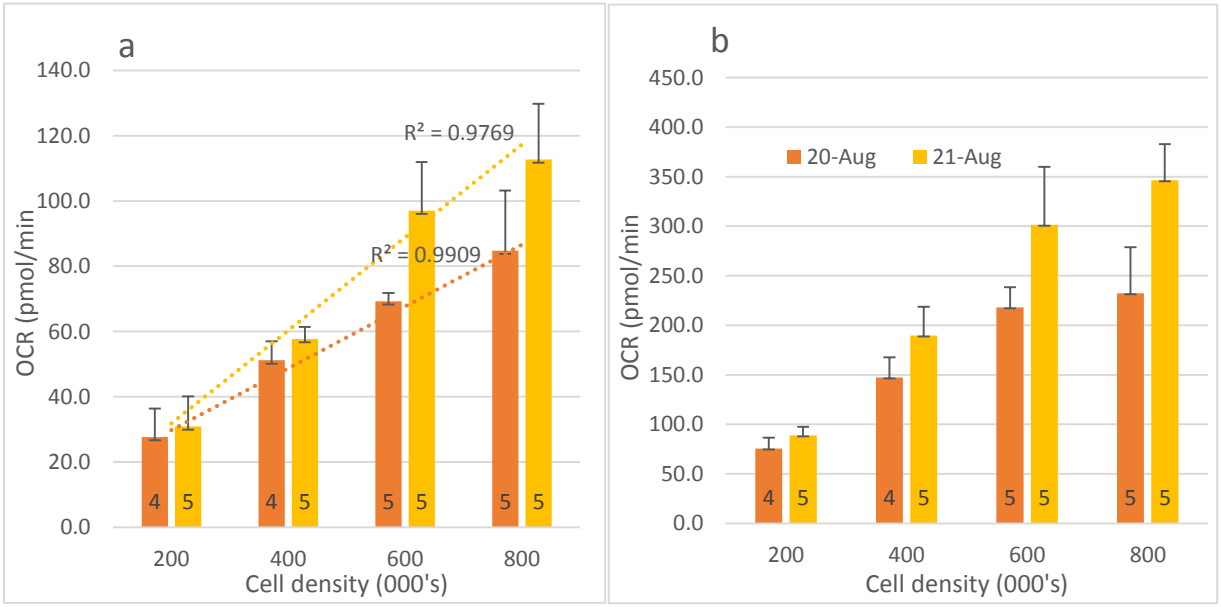


***Figure 3.20 T cell mitochondrial stress test optimisation assay.*** *(a) basal and (b) maximal respiration for T cells from two donors. Oli = 0.60 µM, FCCP = 0.6µM, Ama = 10 µM. Data represent mean values from 4-5 wells ± standard deviation.*

Basal respiration displayed a linear response to increasing cell densities between 2 x $10^5$ and 8 x $10^5$ cells per well. The OCR values over this range are marginally low for the

instrument's sensitivity. Maximal respiration appears to increase in a linear fashion in the range of 2 x $10^5$ and 6 x $10^5$ cells per well. This relative increase appears to cease at higher densities of 8 x $10^5$ cells per well. Visually, T cells appear confluent at a density of 6 x $10^5$ cells per well (Figure 3.21). Based on these findings the density of 6 x $10^5$ T cells per well was chosen as the highest optimal seeding density for future experiments.

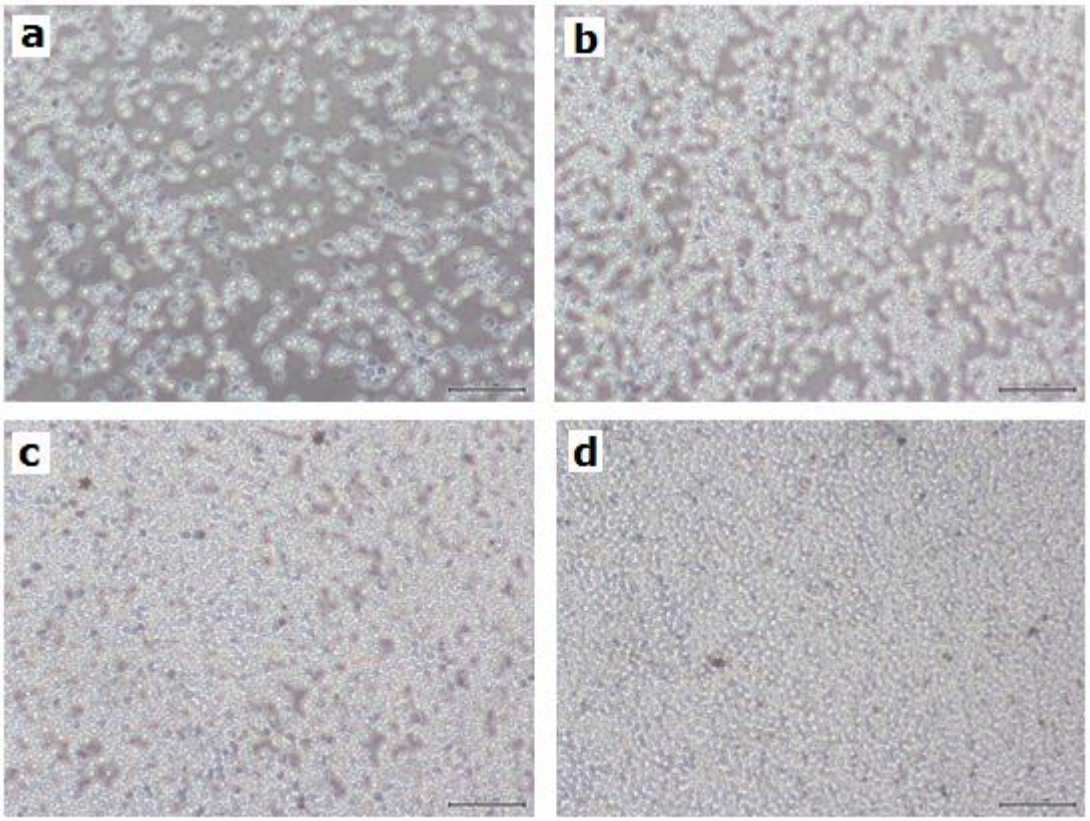


***Figure 3.21 Microscopic images of varying T cells densities.*** *Cells plated in a XF24 cell microplate. Densities are as follows: a) 2*$10^5$*, b) 4*$10^5$*, c) 6*$10^5$*, d) 8*$10^5$*.*

Results from two FCCP optimisation assays (Figure 3.22) show a non-linear concentration response in OCR with a slope of the line decreasing at higher dose concentrations. A concentration of 1 mM was chosen as the optimal dose to achieve maximal OCR and to lessen the impact on OCR of small variations in drug concentrations that may persist between experiments.

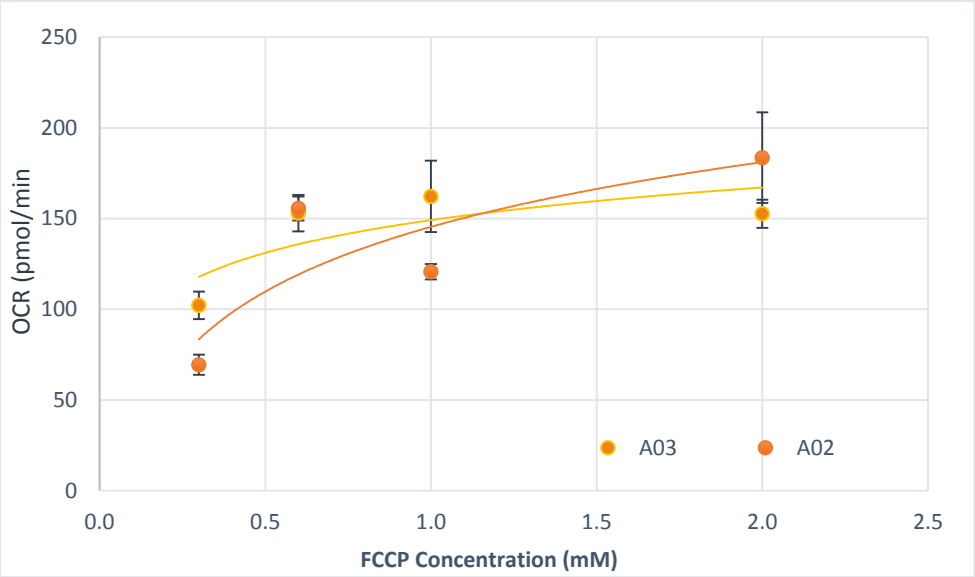


***Figure 3.22 T cell FCCP Response - Reserve Capacity.*** *Reserve capacity is shown for T cells from two donors (A02, A03). Oli = 0.60 µM, FCCP = varied, Ama = 10 µM. Data represent mean values from 3-5 wells ± standard deviation.*

The purity of T cell preparations was tested using CD3-PE monoclonal antibody incubation and flow cytometric detection (Figure 3.23). The average cell preparation contained ~90% T cells with ~10% contamination of lymphocytes that are not T cells.

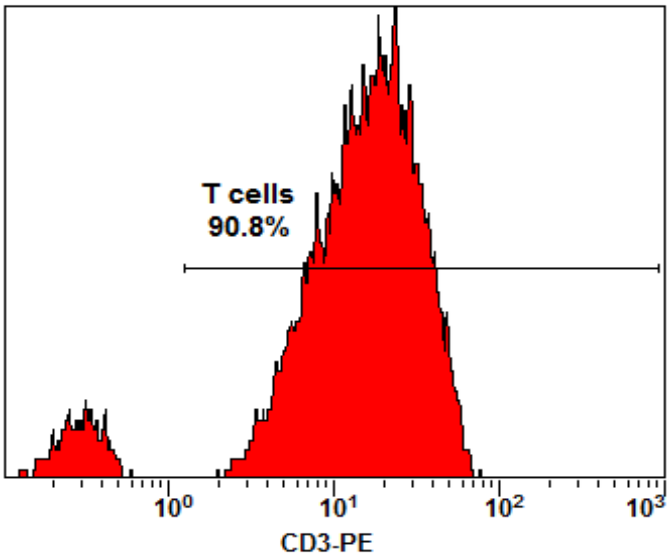


***Figure 3.23 Flow cytometry analysis of purified T cells using CD3-PE mAb labelling.***

Representative results from a T cell optimisation experiment are shown in Figure 3.24. Here the bioenergetics trace is given for a cell seeding density experiment. The OCR values are normalised to cell number ($10^5$ cells per well) and the various densities are grouped into a single data set. Of the 20 wells assayed, 9 were ultimately excluded as abnormal wells or outliers. The reserve capacity of T cells is very evident in the raw trace and is quantified in Figure 3.25, which shows each bioenergetics parameter as a percentage of basal respiration.

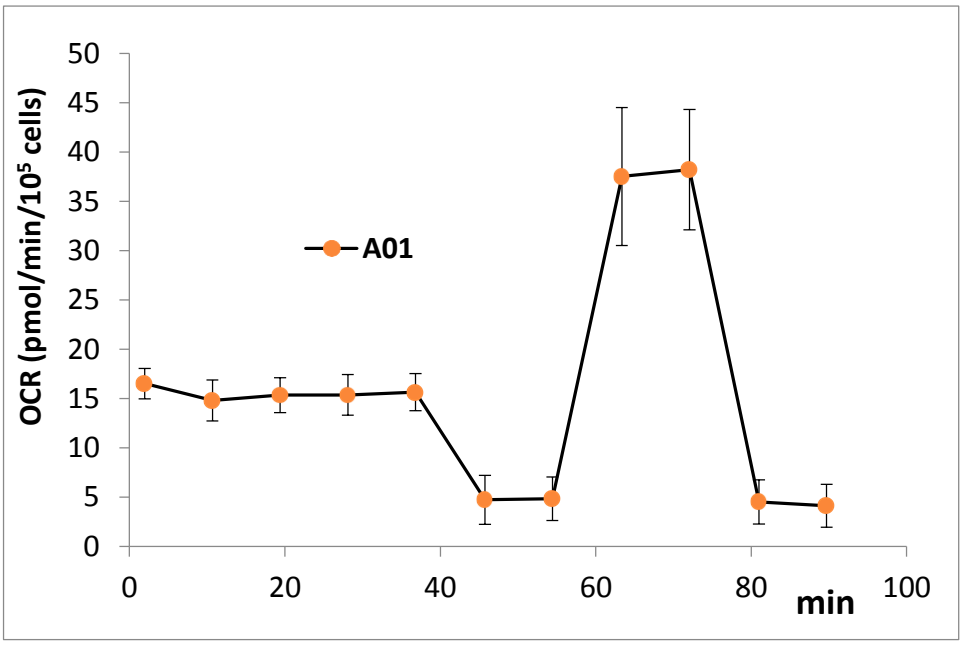


***Figure 3.24 Representative bioenergetics trace of a T cell mitochondrial stress test.*** *Donor A01. Normalised to $10^5$ cells per well. Oli = 0.6 µM, FCCP = 0.6µM, Ama = 10 µM. Data represent mean values from 11 wells ± standard deviation.*

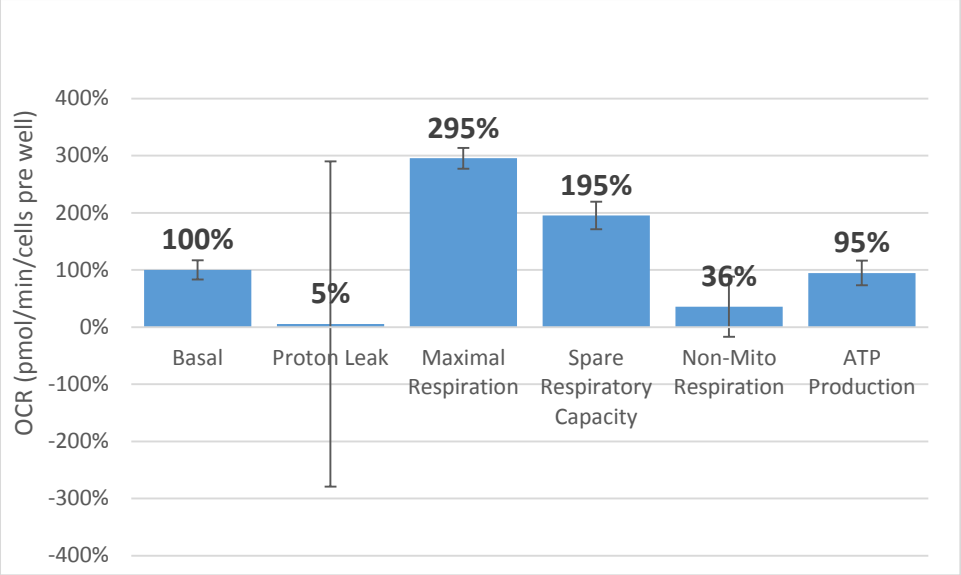


***Figure 3.25 T cell bioenergetic parameters - % of basal.*** *Donor A01. Normalised to $10^5$ cells per well. Oli = 0.6 µM, FCCP = 0.6µM, Ama = 10 µM. Data represent mean values from 11 wells ± standard deviation.*

A demonstration of a T cell BHI valuation is given in Figure 3.26, which shows the BHI for the same experiment shown in Figures 3.21 and 3.22. Again, the exponents for each parameter of the equation are set to one.

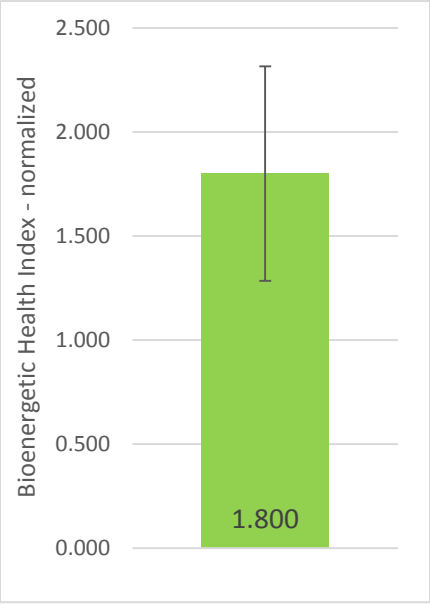


***Figure 3.26 Representative T cell BHI.*** *A single metric encompassing four T cell bioenergetic parameters measured by the mitochondrial stress test. Donor A01, n =11 ± standard deviation.*

# Chapter Four: Discussion

In an effort to measure mitochondrial function in circulating blood cells I trialled three isolation and purification techniques to prepare cell solutions for XF analysis. Following successful isolation, platelets and T cells were assayed by the mitochondrial stress test to reveal their characteristic bioenergetic parameters as determined indirectly by the dynamic measurement of oxygen consumption rates under experimentally controlled conditions.

## 4.1 Summary of results

### 4.1.1 Cell Isolations

Both platelets and T cells were successfully isolated and purified from freshly drawn blood within 3-4 hours of collection. $PGI_2$, through its inhibition of platelet activation allowed repeated rounds of centrifugation and re-suspension without aggregation occurring, and sufficient platelets were purified from 9 ml of blood to seed 5-6 wells at 40 x $10^6$ platelets per well. T cells were purified through negative selection to yield a ~90% pure cell isolate. This is in line with purity results reported in similar protocols (51). EDTA vacuum tubes showed no observed effect on cells bioenergetics consistent with prior reports (56). Nine ml of whole blood produced enough T cells to seed 6-7 wells. Both platelets and T-cells displayed a homogenous monolayer when plated onto XF cell plates before commencement of the mitochondrial stress test.

Attempts to follow a recently published protocol for the isolation of platelets, monocytes and lymphocytes from the same blood collection was unsuccessful due to the failure to produce suitably pure isolations (56). It was found that the PRP centrifugation step had an undesirable effect on Ficoll density separation and resulted in neutrophil contamination through all layers of the Ficoll separation. The positive selection for monocytes using magnetic bead labelled antiCD14 antibodies and MACS separation failed

to adequately elute away lymphocytes. The presence of lymphocytes in the CD14 positive flow-through collection may be due to activation of lymphocytes in the presence of monocytes. Activation can cause CD14 antigenicity in the lymphocytes (57) and if this change occurs it becomes redundant to positively select monocytes by using CD14 positive selection from a PBMC mixture. This result brought into question the merit of using CD14 positive selection to achieve pure isolations of monocytes. It has been previously reported that the CD14 antigen is not solely unique to this cell type (58). It was decided that rather than isolating all three cell types by one continuous preparation as the protocol set forth, it was more advantageous to conduct individual cell preparations.

### 4.1.2 Unexpected Results

Both platelet and T cell XF assays experienced loss of data due to the exclusion of wells that displayed uncharacteristic bioenergetics OCR or ECAR traces. Throughout the 12 platelet experiments it became evident that these unexpected results could be categorised by four patterns and that criterion 1 was the most frequently occurring. While the other three classifications could be accepted as outliers due to random and infrequent occurrence, that was not the case for criterion 1. In these wells it appeared that the cell population switched energy metabolism to make a much greater use of glycolysis. The metabolic switching was seen to occur independent of cell density, glutamine, extracellular media concentration or pH. It was also seen to occur in a non-random fashion, typically occurring in groups in one area of the cell plates despite the plating being carried out in with a multipipette. All wells began with homogenous and confluent cell monolayers but many displayed varying degrees of clumping by the end of the assay. Some evidence of platelet aggregation was seen at the conclusion of the experiment however normal wells also exhibited aggregation on many occasions so this was not a phenomenon only seen in criterion 1 wells. By the conclusion of the assay all modulating drugs had been injected into the XF media and these may be influencing the appearance of cells when examined under microscope.

There is a possibility that the experimental conditions may have caused activation of platelets in abnormal wells classified as criterion 1. This is a surprising outcome that is

contrary to some reports. Most notably, Cardenes *et al.* showed that the percentage of activated platelets did not change from before to after the XF assay and they concluded that XF measurement did not stimulate platelet activation (44). It is worth noting that this group uniquely uses an erythrocyte lysis buffer during their cell isolation. Red blood cells (RBCs) are known to enhance platelet reactivity (59) and so this additional precautionary step may be prudent in case of RBC contamination. Similarly, Chacko *et al.* used an activated control group to test for platelet activation during the preparation stage and found that platelets and PBMCs showed no evidence of activation (51). In this same paper the number of replicates varied from 3-5 per group and leads one to suspect some wells may also have required exclusion. This same paper also mentions that artificial activation can result in clumping of cells but gives no record of this occurrence. The risk of platelet activation is also mentioned by Kramer *et al.* who suggest platelets be allowed to sit longer between the PRP isolation and the rest of the purification stages (51). Despite the occasional mention of the risks of platelet activation none of these papers detail any occurrence of outlier wells or mention the exclusion of abnormal wells of any form.

The bioenergetics traces for criterion 1 show an early and definite switch to glycolysis as seen by a rapid increase in ECAR coupled with a sudden decline in OCR. A paper released this year looking at the metabolic plasticity of platelets provide insight into what may be occurring (49). Here the author shows that thrombin induced activation of platelets stimulates both OXPHOS (25%) and GL (300%). This documented increase in OXPHOS during platelet activation strongly contradicts what was observed to occur in criterion 1 wells. This paper explains how platelets are able to make a compensatory switch between metabolic systems and that platelets displaying metabolic plasticity during resting state and thrombin induced activation. As well as D-glucose and pyruvate, platelets have the ability to use both fatty acids (60) and L-glutamine (61) as fuel to provide substrates for the TCA cycle via beta-oxidation and glutaminolysis respectively. Ravi *et al.* also showed that when these two metabolic systems are excluded, whether it be by inhibition or substrate depletion, platelets are able to compensate by generating ATP entirely through glycolysis (49). I believe this may be occurring in the case of criterion 1 wells. Platelet activation may not necessarily be occurring but the platelets metabolic elasticity is allowing a metabolic switch from OXPHOS to glycolysis. This switch seems to be induced by the early measurement cycle and leads me to speculate that the formation of the 7 µl

microchamber may be limiting substrate availability over the four minute measurement period and may be triggering the metabolic switch to glycolysis. This may be overcome by experimentally titrating substrate concentrations to find the level required to ensure they each remain in excess during the formation of the transient microchamber. Failing this, another option would be to trial shorter time periods of measurement, however this goes against manufacturer's recommendations.

### 4.1.3 Optimisation of Experimental Conditions

Following successful cell isolations, optimisation XF assays were conducted on platelets and T cells to determine the optimal values of important experimental condition such as seeding density, FCCP concentration and glutamine supplementation.

The importance of optimising glutamine (GLN) within the extracellular media was only realised after the release in April of a recent study by Ravi *et al*. (49). Here it is shown that GLN depletion from media resulted in significant effect on platelet bioenergetics. Before this paper no additional GLN was added when making up the XF-DMEM media, other than the 2 mM GLN present in XF assay medium. By late in the year we had XF base medium available (which does not contain any GLN) however all GLN assays were carried out prior to this with medium already containing 2 mM GLN. The research by Ravi *et al*. showed that bioenergetics parameters (basal, ATP linked, proton leak, maximal and reserve capacity) all have lower measured OCRs when the assay medium is depleted of GLN, and that all bioenergetics parameters achieve maximal OCR measures with 4 mM of GLN supplementation. Plasma contains between 500-750 μM of GLN (62) meaning optimal concentrations of GLN for XF analysis is ~8 fold higher. The platelet optimisation results (Section 3.1.3) show maximal OCR values for basal respiration after 4 mM of additional GLN has been added, making the total GLN supplementation 6 mM. This 2 mM excess suggests the quality or availability of the 2 mM GLN inherent in the purchased medium may be questionable. The reserve capacity results showed a GLN concentration response in one of three experiments and in one experiment the maximal response was achieved when a total of 4 mM GLN was present in agreeance with the findings of Ravi *et*

*al*. As with all optimisation results the inconsistent number of replicates available is a major hindrance to meaningful interpretation and further assays are needed to conclusively test both the quality of GLN used and the concentration response. Until this time 4 mM GLN total supplementation will continue to be followed.

The need to optimise conditions in order to both maximise measured bioenergetics parameters and to minimise system variation in measurement is of great importance when comparing results from separate research groups. A summary of the critical experimental conditions of the leading researchers in this field is provided in Table 4.1. GLN supplementation is only performed by Chacko and Ravi, with all other groups not including GLN in the XF medium or optimising its concentration. Similar inconsistencies are seen in glucose (GLU) supplementation, equilibration time, FCCP concentration and cell density.

Cell density optimisation experiments led to the conclusion that 40 x $10^6$ platelets and 60 x $10^4$ T cells should be seeded into each well. These values are higher than the average with Cardenes *et al*. being the only other group to use more than 25 x $10^6$ platelets per well. They showed that basal and maximal respiratory rates were dependant on seeding density and OCR showed a linear response between 5-100 x $10^6$ platelets per well and consequently chose 50 x $10^6$ as their seeding density. We observed a similar linear response (Figure 3.16) however in two of three assays this linearity only held at lower seeding densities. Lower OCR was recorded at higher densities of 80 x $10^6$ platelets per well. A similar effect was observed in T cell experiments (Figure 3.20). This reduction in OCR is possibly due to the loss of cells to the extracellular media during repeated rounds of measurement, or a reduction of OXPHOS caused by proximity of platelets to one another in the over-confluent wells.

Optimisation experiments showed that abnormal results were occurring independently of these optimisation parameters. It is understandable that each research facility will display variation in optimal parameters and our particular values chosen, while different, are still similar to those used in other research groups.

***Table 4.1 Summary of experimental conditions for XF assays using blood cells.***

| | Cells | Normalisation | GLU mM | GLN mM | Density /well | FCCP µM |
|---|---|---|---|---|---|---|
| Fink, 2012 | Platelets | Cell number | - | - | $20 \times 10^6$ | 2 |
| Chacko, 2013 | PBMCs | Protein | 5.5 | 4 | $25 \times 10^4$ | 0.6 |
| Chacko, 2013 | Platelets | Protein | 5.5 | 4 | $25 \times 10^6$ | 0.6 |
| Cardenes, 2014 | Platelets | Cell number | 5 | - | $50 \times 10^6$ | 0.7 |
| Kramer, 2014 | Leukocyte | Protein | - | - | $25 \times 10^4$ | 0.6 |
| Kramer, 2014 | Platelets | Protein | - | - | $25 \times 10^6$ | 0.6 |
| Ravi, 2015 | Platelets (96 well) | Protein | 5.5 | 4 | $10 \times 10^6$ | 0.6 |
| Xu, 2015 | Platelets | Cell number | 25 | 2 | $25 \times 10^6$ | 0.7 |

### 4.1.4 Preliminary Results

Results from similar experiments are limited to a few studies and variations in experimental conditions and protocols used make comparison between studies difficult. In other studies normalisation of experimental results has been made by representing OCR values either per μg of protein or per cell number (Table 4.1). My attempts to optimise platelet experiments by protein assay (Methods 2.2.4) failed to suitably reduce well-to-well variation or to accurately determine the protein content of every well. The protein assay resulted in increased data variation and further exclusions due to abnormal results meant that normalising each well to protein content was inexpedient. As such, I chose to normalise data to cell number and to represent bioenergetic parameters as a percentage of basal respiration to counteract any variation in cell seeding number that may occur between experiments. More direct comparisons can be drawn with those that also used cell number to normalise results. Cardenes *et al*. showed that platelets seeded at 50 x $10^6$ cells per well had absolute basal OCR values ~92 pmol $O_2$/min. This is much lower than measurements recorded in platelet optimisation experiments (Section 3.1.3) which typically measured around 200-300 pmol $O_2$/min. Fink *et al*. using 20 x $10^6$ platelets per well measured basal OCR around 120 pmol $O_2$/min which if adjusted to cells number would be in agreeance with my measurements. Kramer *et al*. using densities of 25 x $10^6$ platelets, also gives average basal values of 200 ± 20 pmol $O_2$/min. Their results are also normalised to cell number but has no added glutamine to the assay medium.

Platelet reserve capacity is known to be characteristically low when compared to other cell types (51). Successful optimisation of both FCCP and GLN was needed to consistently produce positive values of reserve capacity. Figure 3.6 shows a representative experiment where reserve capacity was measured as 26% of basal respiration. This is in agreeance with Fink *et al*. who also show reserve capacity of 25% and is similar to the 18% presented by Chacko *et al*. Other studies, such as Xu *et al*. (48) failed measure any reserve capacity in platelets which maybe reflective of the insufficient optimisation experiments on their behalf.

Overall these results agree in part with published studies. The desired bioenergetics parameters were successfully measured and in some instances a BHI was calculated. The BHI was conceived by Chacko *et al*. with the rationale that measured biometric parameters can be grouped to represent positive and negative aspects of bioenergetics function, and then fitted into an index equation accordingly (28). The index was then tested under the influence of a strong oxidative stressor to ensure the metric displays the correct responsiveness to detrimental condition. Each parameter is given an exponent which in the default form is set to 1. The authors suggest that weightings could be applied to each exponent based on biological significance or pathological relevance of the underlying condition being measured. While BHI data is beginning to be published (47, 63) until uniformity in calculation and protocol design is adopted, direct comparisons cannot be drawn between studies. The variability in results that I observed in this study also suggests that there may be a significant problem in standardizing BHI obtained between labs. This reiterates the need to carefully optimise experimental conditions and to maintain consistency and uniformity in protocol to allow making comparisons possible. Once this consistency is achieved, metrics like the BHI may be used to make fast and non-ambiguous comparisons between individuals and between separate studies.

## 4.2 Strengths and limitations

The greatest limitation in this study was the limited number of wells in which to perform the XF assay. The Seahorse instrument available uses 24-well cell-plates and 4 of which are needed to assess background conditions of the experiment. Optimisation experiments ideally required groups of 5 wells for each variable, such as FCCP concentration, limiting the assay to only 4 groups per experiment. On too many occasions a group which contained 5 replicates was reduced to less than 3 due to the problems experienced with exclusion of abnormal results. This was the main hindrance in being able to successfully replicate results in order to be confident the result was optimal. Ravi *et al*. recently used a Seahorse XF96 instrument which uses a 96 well plate which provides much greater

scope to deal with omission of abnormal results and allows for more variables to be compared within a one experiment.

## 4.3 Future Directions

Until the abnormal results problem is addressed it is not possible to generate high quality reproducible results. If metabolic switching is being triggered by substrate limitations during the formation of the microchamber then one possibility would be to lessen the current measurement time. The measurement period of four minutes is recommended by the instruments instruction manual based on the sensitivity of the fluorometric probes and the absolute OCR values that are typically being produced by platelets and PBMCs.

Using an erythrocyte lysis buffer during the platelet preparation may also be advised to try prevent the occurrence of criterion 1 s well as using XF base medium. Testing of the supplements such as GLN and GLU may be necessary to ensure quality and consistency of conditions.

Once the protocol has been successfully developed then it should be tested on a positive control group with diagnosed mitochondrial dysfunction to see if it is capable of detecting mitochondrial dysfunction.

## 4.4 Conclusions

Platelets and T cells continue to demonstrate potential as quick and easily accessed cells from which to measure human mitochondrial function in intact human cells. My research supports others findings that blood cells such as platelets and lymphocytes each have a distinct and measurable set of biometric parameters. Given optimal, uniform and consistent experimental parameters this methodology should be able to quickly assay a large cohort of people. It is not yet clear whether measuring multiple bioenergetics parameters and representing these as a single metric may allow for detection of mitochondrial dysfunction or whether age related variation may be observed.

# References

1. Henze K, Martin W. Evolutionary biology: essence of mitochondria. Nature. 2003;426(6963):127-8.

2. Gray MW, Burger G, Lang BF. Mitochondrial evolution. Science. 1999;283(5407):1476-81.

3. Alberts B, Bray D, Lewis J, Raff M, Roberts K, Watson JD. Molecular biology of the cell. 1994. Garland, New York.139-94.

4. Herst PM, Tan AS, Scarlett D-JG, Berridge MV. Cell surface oxygen consumption by mitochondrial gene knockout cells. Biochimica et Biophysica Acta (BBA)-Bioenergetics. 2004;1656(2):79-87.

5. Hamanaka RB, Chandel NS. Mitochondrial reactive oxygen species regulate cellular signaling and dictate biological outcomes. Trends in biochemical sciences. 2010;35(9):505-13.

6. Butow RA, Avadhani NG. Mitochondrial signaling: the retrograde response. Molecular cell. 2004;14(1):1-15.

7. Stumpf DA, Haas R, Eguren LA, Parks JK, Eilert RE. Protonmotive force in muscle mitochondria. Muscle & nerve. 1982;5(1):14-9.

8. Qian W, Van Houten B. Alterations in bioenergetics due to changes in mitochondrial DNA copy number. Methods. 2010;51(4):452-7.

9. Lemasters JJ. Selective mitochondrial autophagy, or mitophagy, as a targeted defense against oxidative stress, mitochondrial dysfunction, and aging. Rejuvenation research. 2005;8(1):3-5.

10. Lin MT, Beal MF. Mitochondrial dysfunction and oxidative stress in neurodegenerative diseases. Nature. 2006;443(7113):787-95.

11. Miller FJ, Rosenfeldt FL, Zhang C, Linnane AW, Nagley P. Precise determination of mitochondrial DNA copy number in human skeletal and cardiac muscle by a PCR-based assay: lack of change of copy number with age. Nucleic acids research. 2003;31(11):e61-e.

12. Baker MJ, Frazier AE, Gulbis JM, Ryan MT. Mitochondrial protein-import machinery: correlating structure with function. Trends in cell biology. 2007;17(9):456-64.

13. Wallace DC, Ye J, Neckelmann SN, Singh G, Webster KA, Greenberg BD. Sequence analysis of cDNAs for the human and bovine ATP synthase β subunit: mitochondrial DNA genes sustain seventeen times more mutations. Current genetics. 1987;12(2):81-90.

14. Balaban RS, Nemoto S, Finkel T. Mitochondria, oxidants, and aging. Cell. 2005;120(4):483-95.

15. Duchen MR. Mitochondria in health and disease: perspectives on a new mitochondrial biology. Molecular aspects of medicine. 2004;25(4):365-451.

16. Zeevalk G, Bernard L, Song C, Gluck M, Ehrhart J. Mitochondrial inhibition and oxidative stress: reciprocating players in neurodegeneration. Antioxidants & redox signaling. 2005;7(9-10):1117-39.

17. Kramer PA, Darley-Usmar VM. The Emerging Theme of Redox Bioenergetics in Health and Disease. Biomedical journal. 2015.

18. Bergamini E, Cavallini G, Donati A, Gori Z. The role of macroautophagy in the ageing process, anti-ageing intervention and age-associated diseases. The international journal of biochemistry & cell biology. 2004;36(12):2392-404.

19. Shi C, Guo K, Yew DT, Yao Z, Forster EL, Wang H, et al. Effects of ageing and Alzheimer's disease on mitochondrial function of human platelets. Experimental gerontology. 2008;43(6):589-94.

20. Cui H, Kong Y, Zhang H. Oxidative stress, mitochondrial dysfunction, and aging. Journal of signal transduction. 2011;2012.

21. Camougrand N, Kiššová I, Velours G, Manon S. Uth1p: a yeast mitochondrial protein at the crossroads of stress, degradation and cell death. FEMS yeast research. 2004;5(2):133-40.

22. Copeland WC. Inherited mitochondrial diseases of DNA replication. Annual review of medicine. 2008;59:131.

23. DiMauro S, Davidzon G. Mitochondrial DNA and disease. Annals of medicine. 2005;37(3):222-32.

24. Petty R, Harding A, Morgan-Hughes J. The clinical features of mitochondrial myopathy. Brain. 1986;109(5):915-38.

25. Polyak K, Li Y, Zhu H, Lengauer C, Willson JK, Markowitz SD, et al. Somatic mutations of the mitochondrial genome in human colorectal tumours. Nature genetics. 1998;20(3):291-3.

26. Chinnery PF, Samuels DC, Elson J, Turnbull DM. Accumulation of mitochondrial DNA mutations in ageing, cancer, and mitochondrial disease: is there a common mechanism? The Lancet. 2002;360(9342):1323-5.

27. Hauptmann S, Keil U, Scherping I, Bonert A, Eckert A, Müller WE. Mitochondrial dysfunction in sporadic and genetic Alzheimer's disease. Experimental gerontology. 2006;41(7):668-73.

28. Chacko BK, Kramer PA, Ravi S, Benavides GA, Mitchell T, Dranka BP, et al. The Bioenergetic Health Index: a new concept in mitochondrial translational research. Clinical Science. 2014;127(6):367-73.

29. Widlansky ME, Wang J, Shenouda SM, Hagen TM, Smith AR, Kizhakekuttu TJ, et al. Altered mitochondrial membrane potential, mass, and morphology in the mononuclear cells of humans with type 2 diabetes. Translational Research. 2010;156(1):15-25.

30. Ren J, Pulakat L, Whaley-Connell A, Sowers JR. Mitochondrial biogenesis in the metabolic syndrome and cardiovascular disease. Journal of Molecular Medicine. 2010;88(10):993-1001.

31. Wu M, Neilson A, Swift AL, Moran R, Tamagnine J, Parslow D, et al. Multiparameter metabolic analysis reveals a close link between attenuated mitochondrial bioenergetic function and enhanced glycolysis dependency in human tumor cells. American Journal of Physiology-Cell Physiology. 2007;292(1):C125-C36.

32. LEE HC, YIN PH, LIN JC, WU CC, CHEN CY, WU CW, et al. Mitochondrial genome instability and mtDNA depletion in human cancers. Annals of the New York Academy of Sciences. 2005;1042(1):109-22.

33. Brand M, Nicholls D. Assessing mitochondrial dysfunction in cells. Biochem J. 2011;435:297-312.

34. Brand MD, Chien L-F, Diolez P. Experimental discrimination between proton leak and redox slip during mitochondrial electron transport. Biochem J. 1994;297:27-9.

35. Clark LC, Wolf R, Granger D, Taylor Z. Continuous recording of blood oxygen tensions by polarography. Journal of applied physiology. 1953;6(3):189-93.

36. Chance B, Williams G. Respiratory enzymes in oxidative phosphorylation I. Kinetics of oxygen utilization. Journal of Biological Chemistry. 1955;217(1):383-94.

37. Scott I, Nicholls D. Energy transduction in intact synaptosomes. Influence of plasma-membrane depolarization on the respiration and membrane potential of internal mitochondria determined in situ. Biochem J. 1980;186:21-33.

38. Nobes C, Brown GC, Olive PN, Brand MD. Non-ohmic proton conductance of the mitochondrial inner membrane in hepatocytes. Journal of Biological Chemistry. 1990;265(22):12903-9.

39. Jekabsons MB, Nicholls DG. In situ respiration and bioenergetic status of mitochondria in primary cerebellar granule neuronal cultures exposed continuously to glutamate. Journal of Biological Chemistry. 2004;279(31):32989-3000.

40. Deshpande RR, Heinzle E. On-line oxygen uptake rate and culture viability measurement of animal cell culture using microplates with integrated oxygen sensors. Biotechnology letters. 2004;26(9):763-7.

41. Gnaiger E, Steinlechner-Maran R, Méndez G, Eberl T, Margreiter R. Control of mitochondrial and cellular respiration by oxygen. Journal of bioenergetics and biomembranes. 1995;27(6):583-96.

42. Fern R. Variations in spare electron transport chain capacity: The answer to an old riddle? Journal of neuroscience research. 2003;71(6):759-62.

43. Avila C, Huang R, Stevens M, Aponte A, Tripodi D, Kim K, et al. Platelet mitochondrial dysfunction is evident in type 2 diabetes in association with modifications of mitochondrial anti-oxidant stress proteins. Experimental and clinical endocrinology &

diabetes: official journal, German Society of Endocrinology [and] German Diabetes Association. 2012;120(4):248-51.

44. Cardenes N, Corey C, Geary L, Jain S, Zharikov S, Barge S, et al. Platelet bioenergetic screen in sickle cell patients reveals mitochondrial complex V inhibition, which contributes to platelet activation. Blood. 2014;123(18):2864-72.

45. Fink BD, Herlein JA, O'Malley Y, Sivitz WI. Endothelial cell and platelet bioenergetics: effect of glucose and nutrient composition. PloS one. 2012;7(6):e39430.

46. Zharikov S, Shiva S. Platelet mitochondrial function: from regulation of thrombosis to biomarker of disease. Biochem Soc Trans. 2013;41(1):118-23.

47. Ravi S, Chacko B, Kramer PA, Sawada H, Johnson MS, Zhi D, et al. Defining the effects of storage on platelet bioenergetics: The role of increased proton leak. Biochimica et Biophysica Acta (BBA)-Molecular Basis of Disease. 2015;1852(11):2525-34.

48. Xu W, Cardenes N, Corey C, Erzurum SC, Shiva S. Platelets from Asthmatic Individuals Show Less Reliance on Glycolysis. PloS one. 2015;10(7):e0132007.

49. Ravi S, Chacko B, Sawada H, Kramer PA, Johnson MS, Benavides GA, et al. Metabolic Plasticity in Resting and Thrombin Activated Platelets. PloS one. 2015;10(4).

50. Hartman M-L, Shirihai OS, Holbrook M, Xu G, Kocherla M, Shah A, et al. Relation of mitochondrial oxygen consumption in peripheral blood mononuclear cells to vascular function in type 2 diabetes mellitus. Vascular Medicine. 2014;19(1):67-74.

51. Chacko BK, Kramer PA, Ravi S, Johnson MS, Hardy RW, Ballinger SW, et al. Methods for defining distinct bioenergetic profiles in platelets, lymphocytes, monocytes, and neutrophils, and the oxidative burst from human blood. Laboratory Investigation. 2013;93(6):690-700.

52. Kramer PA, Ravi S, Chacko B, Johnson MS, Darley-Usmar VM. A review of the mitochondrial and glycolytic metabolism in human platelets and leukocytes: Implications for their use as bioenergetic biomarkers. Redox biology. 2014;2:206-10.

53. Kramer PA, Chacko BK, Ravi S, Johnson MS, Mitchell T, Darley-Usmar VM. Bioenergetics and the Oxidative Burst: Protocols for the Isolation and Evaluation of

Human Leukocytes and Platelets. JoVE (Journal of Visualized Experiments). 2014(85):e51301-e.

54. Walkowiak B, Kęsy A, Michalec L. Microplate reader-a convenient tool in studies of blood coagulation. Thrombosis research. 1997;87(1):95-103.

55. Gryglewski RJ. Prostacyclin among prostanoids. Pharmacol Rep. 2008;60(1):3-11.

56. Kramer PA, Chacko BK, Ravi S, Johnson MS, Mitchell T, Darley-Usmar VM. Bioenergetics and the oxidative burst: protocols for the isolation and evaluation of human leukocytes and platelets. Journal of visualized experiments: JoVE. 2014(85).

57. Fridlender ZG, Rabinowitz R, Schlesinger M. Monocytes confer CD14 antigenicity on activated lymphocytes. Human immunology. 1999;60(11):1028-38.

58. Jersmann HP. Time to abandon dogma: CD14 is expressed by non-myeloid lineage cells. Immunology and cell biology. 2005;83(5):462-7.

59. Santos M, Valles J, Marcus A, Safier L, Broekman M, Islam N, et al. Enhancement of platelet reactivity and modulation of eicosanoid production by intact erythrocytes. A new approach to platelet activation and recruitment. Journal of Clinical Investigation. 1991;87(2):571.

60. Majerus PW, Smith M, Clamon G. Lipid metabolism in human platelets: I. Evidence for a complete fatty acid synthesizing system. Journal of Clinical Investigation. 1969;48(1):156.

61. Vasta V, Meacci E, Farnararo M, Bruni P. Glutamine transport and enzymatic activities involved in glutaminolysis in human platelets. Biochimica et Biophysica Acta (BBA)-General Subjects. 1995;1243(1):43-8.

62. Bassit RA, Sawada LcA, Bacurau RF, Navarro F, Martins E, Santos RV, et al. Branched-chain amino acid supplementation and the immune response of long-distance athletes. Nutrition. 2002;18(5):376-9.

63. Kramer PA, Chacko BK, George DJ, Zhi D, Wei C-C, Dell'Italia LJ, et al. Decreased Bioenergetic Health Index in monocytes isolated from the pericardial fluid and blood of post-operative cardiac surgery patients. Bioscience reports. 2015;35(4):e00237.